國 立 高 雄 應 用 科 技 大 學

電 機 工 程 系

碩 士 論 文

低成本實現心電圖暨 HRV 即時偵測系統

A LOW COST ECG AND HRV DETECTION SYSTEM

研 究 生：陳 穎 儒

指導教授：王 冠 智　博士

中 華 民 國 一 百 零 一 年 七 月

National Kaohsiung University of Applied Sciences

A LOW COST ECG AND HRV DETECTION SYSTEM

by

Ying-Ju Chen

Advised by

Luke K. Wang

A Thesis

Submitted to

Institute of Electrical Engineering

in Partial Fulfillment of the Requirements

for the Degree of Master

in

Electrical Engineering

Kaohsiung, Taiwan, Republic of China

July 2012

國立高雄應用科技大學研究所學位論文考試審定書

本校 電機工程系碩士班

研究生 陳穎儒 所提之論文

低成本實現心電圖暨HRV即時偵測系統

合於 碩士 資格水準，業經本委員會評審認可。

學位考試委員會

召集人 [signature] 簽章

委員 [signature] [signature]

[signature] [signature]

[signature] [signature]

[signature] [signature]

指導教授 [signature] 簽章

系所主管 [signature] 簽章

A LOW COST ECG AND HRV DETECTION SYSTEM

by

Ying-Ju Chen

A Thesis Submitted to the Graduate Division in Partial
Fulfillment of the Requirements for the Degree of
Master of Science in the Department of Electrical Engineering
National Kaohsiung University of Applied Sciences
Kaohsiung, Taiwan, Republic of China
July 23, 2012

Approved by :

Thesis Advisor : Luke C Way

Institute Director : Hsiao-Yi Lee

A LOW COST ECG AND HRV DETECTION SYSTEM

Student：Ying-Ju Chen Advisor：Dr. Luke K. Wang

Department of Electrical Engineering

National Kaohsiung University of Applied Sciences

ABSTRACT

In this paper, we describe a low cost electrocardiogram (ECG) machine with off-the-shelf components implementing the real-time QRS wave which is the main wave of ECG and Heart Rate Variability (HRV) detection. According to the measurement method of Einthoven triangle proposed by Willen Einthoven, we can obtain the ECG signal. We use the ten NT coins as the sensor to catch heart signal, and amplify the weak signals by means of instrumentation amplifier consisting of several operation amplifiers. In order to distinguish the QRS wave clearly, we apply the Sallen-Kay and Notch filter to remove unwanted noises. Using the PC's sound card via the microphone port, we digitize the ECG signal, and show it on the PC monitor. In the PC station, we develop a real-time ECG and HRV monitoring system based on Visual Basic 6.0, and via this system we show the QRS wave and the detection results of HRV. Employing a dynamic threshold to obtain the R wave and number of heart rate decide the R wave position. Via the position distribution of the R wave, we can know whether the patient has the arrhythmia or not. According to this feature transmitted from the distant end by the ZIGBEE in real-time, caregiver can determine whether the patient needs to give first aid or not. Furthermore, the system may increase the survival rate of patients.

KEYWORDS – Electrocardiogram, ZIGBEE, Willem Einthoven, HRV, Sallen-Kay, Notch Filter, QRS, Instrumentation Amplifier.

低成本實現心電圖暨 HRV 即時偵測系統

學生：陳穎儒　　指導教授：王冠智 博士

國立高雄應用科技大學 電機工程系 碩士班

摘　要

本文提出如何運用坊間現成的元件去實現低耗費的心電圖 QRS 波暨心率變異(HRV)的即時偵測。我們運用十元硬幣去當作心電圖的探測器，並透過 Willem Einthoven 所提出之三角量測法去獲得心電訊號，並將所得之訊號透過由運算放大器組成之儀表放大器放大後，再將此含有雜訊的心電訊號透過 Sallen-Kay 低通濾波器及 Notch 市電雜訊濾波器去除，即可獲得足以辨識的 QRS 心電訊號，隨後將心電訊號透過電腦端麥克風接孔傳送到音效卡執行類比-數化轉換，最後將訊號即時的顯示在電腦螢幕上；在電腦端則配置了自行開發之 HRV 暨心電圖即時偵測系統，藉由此系統我們可以將心電訊號的 QRS 波即時的顯示於系統視窗介面上，再透過一動態的心率暨 R 波門檻，即時計算出心率數及 R 波位置，再藉由 R 波位置的變化，即可探測出患者是否有心律失常的特徵，最後再將此特徵記錄下來，並透過無線 ZIGBEE 即時的將危險訊號傳遞至遠處接收端，讓監護者判斷是否有需要進行救護動作，進而提高患者的生存率。

關鍵字－心電圖、ZIGBEE、Willem Einthoven、Sallen-Kay、Notch Filter、QRS、HRV、心律變異、心律失常、儀表放大器、運算放大器、濾波器。

致　謝

很快的在高應大兩年的碩士求學階段已經告一個段落了，在最後一年能夠圓滿完成本論文，首先必須感謝王冠智 老師的用心栽培，有他的悉心指導，讓我真正了解如何作研究是怎一回事，也得知了不少健康相關的知識，讓學生在拼命研究的同時，還能兼顧到身體的健康，真是令我感激不盡；還有在這兩年中，要由衷的感謝 謝勝治老師專業知識及做人處事上的建議，才能讓學生研究所期間能夠迅速的脫離撞牆期，不讓時間白白的浪費掉，也讓學生瞭解對於事情不僅要知其然，還要知其所以然，得讓本論文更臻於完備。

感謝學長蔡政昇、吳建樟、陳文正、王士豪、楊緒屏、藍仁鴻、陳思維、黃存豐、簡贊峰、王正皇、王彥中對我的協助與建議，還有同學黃明益、溫韋翔、杜俊、學弟柯孜澄等，我的研究所生活因為有你們而美麗。

最後要感謝我的父親母親們，感謝你們不辭辛苦的賺錢讓我讀到碩士，曾經好幾次颱風來時，我好想回去幫你們拯救農作物，你們總是會要我好好讀書就好，孰不知你們已經忙的不可開交了，謝謝你們總是這麼的體諒我，讓我可以無憂無慮的作研究。最後感謝我的爺爺和姐姐對我的信任和幫忙，讓我很多事總是這麼順利。在此僅以小小的成果獻給關懷我的人，與你們分享我的喜悅，並獻上最高的謝意。

陳穎儒 謹誌於

高雄應用科技大學電機工程系

中華民國一百零一年七月

CONTENTS

LIST OF FIGURES

LIST OF TABLES

CHAPTER 1

INTRODUCTION

With the global competition, more and more people fall into the overwork situation. Under this kind of environment of high pressure and overwork, many diseases of affluence are suddenly producing in recent year. According to **Table 1-1**, it is listed the "Top 10 Causes of Death" from 2008 to 2011. In this table, we can easily find the heart disease which is ranked first. More information is revealed in WHO about the hi-income and mid-income countries have the higher probability catching a heart disease. On the other hand, the low-income countries have the lower. In Taiwan, the bus drivers often afflicted with the sudden death because they are always overworked. This kind of death has a greatly relationship with the so-called Sudden Cardiac Death (SCD) [Lin, 2007]. Before occurring this fatal disease, both have the common phenomenon which is so-called Arrhythmia [Cardiac Dysrhythmia].

Table 1-1 Top 10 Causes of Death from World Health Organization

World	Deaths in millions	% of deaths
Ischaemic heart disease	7.25	12.8%
Stroke and other cerebrovascular disease	6.15	10.8%
Lower respiratory infections	3.46	6.1%
Chronic obstructive pulmonary disease	3.28	5.8%
Diarrhoeal diseases	2.46	4.3%
HIV/AIDS	1.78	3.1%
Trachea, bronchus, lung cancers	1.39	2.4%
Tuberculosis	1.34	2.4%
Diabetes mellitus	1.26	2.2%
Road traffic accidents	1.21	2.1%

The SCD is usually hard to avoid in real-time, and that is often caused the heavy accident. The **Figure 1-1** illustrates an example of arrhythmia symptom. That makes the interval of heart rate to become longer.

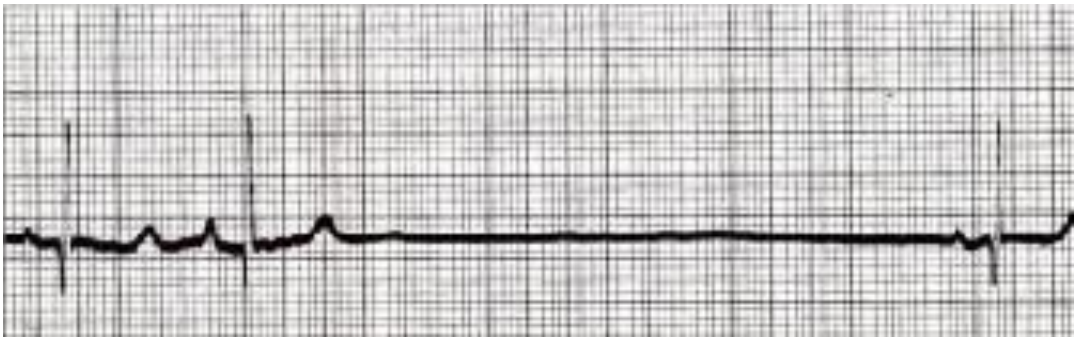

Figure 1-1 Arrhythmia Diagram [YUMAX, 2010]

This symptom is extremely hard to find. There is a way to illustrate this symptom that is so-called Heart Rate Variability (HRV). For healthy adults, their heart rates are between 60 and 80 beats per minute (BPM). Thus, the interval time is around 0.75 sec. If a patient's heart rate is often away this range, the caused probability of SCD is higher than a normal one. When it is occurred, only 1-2 percent patient can survive. If we can employ the common symptom which is the arrhythmia to find the possibility of caused SCD, it will increase the survival rate of patient and reduce the accident rate of traffic. The first ECG machine which is employed to measure the heart biopotential is proposed by Willem Einthoven [Einthoven's Triangle]. This machine draws out ECG on the paper successfully. This typical ECG machine in hospital is usually bigger and inconvenient for general public. [Segura-Juarez et al., 2004] proposed a complete and professional application in ECG machine. They build a Holter which is a small and portable ECG machine. This recorder is battery powered and includes a graphical display and keyboard. That is capable of acquiring up to 48 hours of continuous electrocardiogram data. Regardless of the Holter or typical ECG machine, they are usually expensive and not user-friendly.

We described a complete design of an ECG machine. The design uses off-the shelf components and the total cost is around 100 NT dollars. It is small and compact, and capable of producing more detail information, recording at all time, powered by 9 V battery, HRV detection, etc.

CHAPTER 2

ECG ANALYSIS

This chapter describes the concepts about ECG measurement as follow: Section 2.1 illustrates how the heart work and yield the weak potential by itself. Section 2.2 depicts the measurement method of physiologic signal. Section 2.3 describes how to further amplify the weak physiologic signal. Section 2.4 demonstrates the kind of ECG noise. Section 2.5 expresses how to derivation filter equations. Section 2.6 describes how to design the filters.

2.1 Introduction the Heart

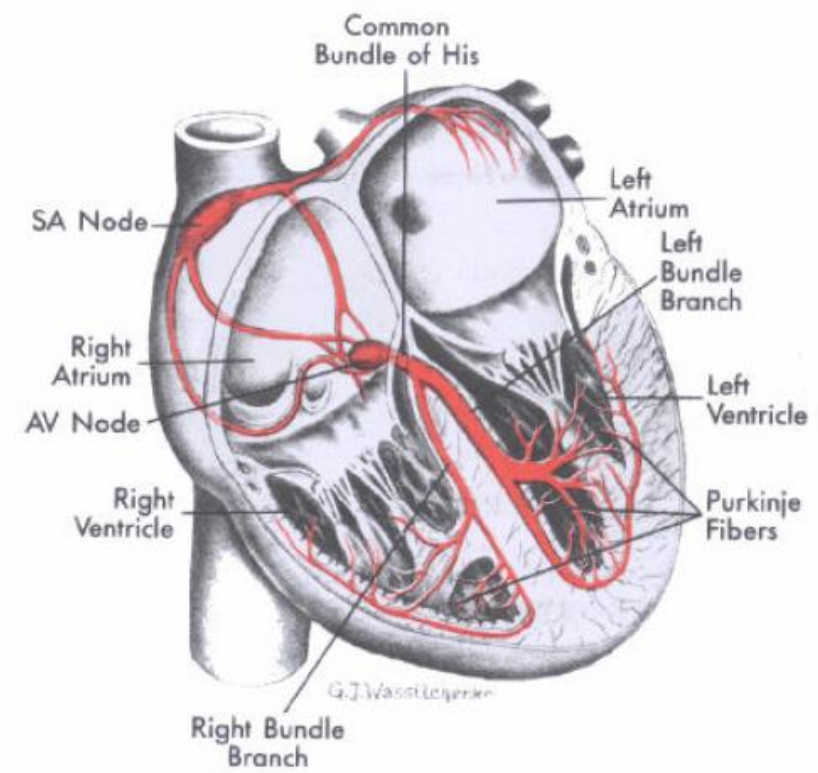

Figure 2-1 The Cardiac Structure [Chang, 2004]

Before measuring the heart signal, we need to know how the heart work and yield biopotential by itself. The heart is roughly separated into right atrium, right ventricle,

left atrium, and left ventricle as shown in **Figure 2-1**. For normal adults, their heart will rhythmic contract about sixty to eighty times per minute over and over again [Chang, 2004]. The contraction action is mainly caused by the Sinoatrial node (SA node) which can self-excitatory [Malmivuo et al., 1995] located upon the right atrium. The SA node generates an impulse signal to the Atrioventricular node (AV node) which is located between the atria and ventricles for activation cells of AV node. The activation propagates from SA node to AV node, and then spreads throughout the heart. The contraction usually follows the process of activation propagation. So, we can realize the contraction activity manipulated by the SA node. A series of activation are described as below (**Figure 2-2**):

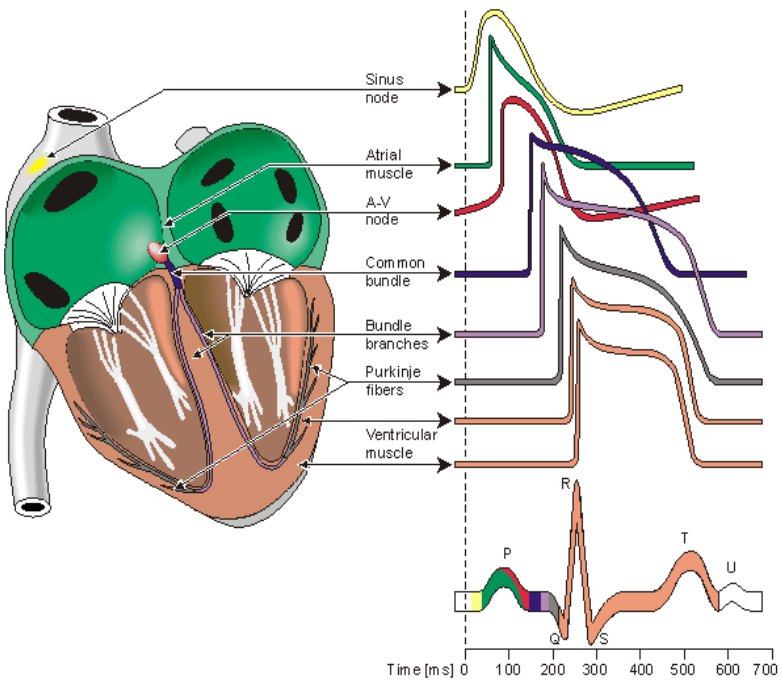

Figure 2-2 Electrophysiology of the Heart [Malmivuo et al., 1995]

The **Figure 2-2** shows the different position of potential activity in heart. They are mixed to produce a PQRST wave which is under the **Figure 2-2**. Every wave records distinct movement respectively as follow:

- *P wave: the sequential activation (depolarization) of the right and left atria.*

- *QRS wave: right and left ventricular depolarization.*
- *T wave: ventricular repolarization.*

In the static situation, the cardiac cell belonging to negatively charged is so-called polarization. Therefore, depolarization is belong to positively charged [Chang, 2004], and then the repolarization means the positively charged come back to the negatively charged. While the cardiac cell is in the process of depolarization, the heart will produce the contraction reaction. Otherwise, when the cardiac cell come back to negatively charged, the heart will occur the diastolic situation. Among the PQRST, the QRS complex is the important feature because they are the most easy to recognize. Through upon explanation, we can know the PQRST wave implying the each movement in the various place of heart described in **Figure 2-3**. By measuring the potential via the ECG sensors from different position of body, we can record variation potential of heart and obtain the so-called ECG.

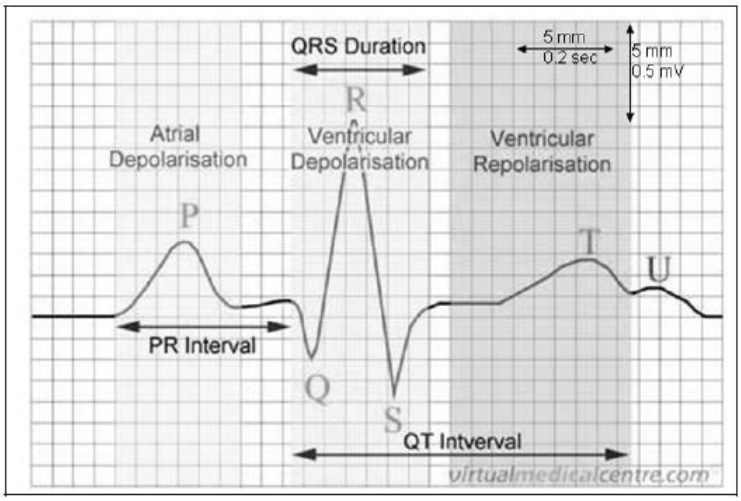

Figure 2-3 Typical ECG with Actions [Wang, 2008]

Usually, the ECG can be measured out from every position of body, but leave away the heart more, and the signal will tiny more. Thus, we can regard the body as a conductor included the resistor, and the blood is the conduct liquid. When measuring the ECG from artifices, the potential is smaller than the potential obtained from chest.

The **Figure 2-4** shows each type of physiological electronic signal [Wang, 2008]. These signals are always useful to the diagnosis of diseases in clinical reference. The **Table 2-1** expresses the physiological signal of amplitude and frequency [Chang, 2004]. According to **Table 2-1**, we need to amplify the signal between 0.02-5 mV, and filter out the signal outside the frequency between 0.05-100 Hz. For obtaining the pure and identifiable ECG signal, the circuit must add in amplification circuit, filter circuit, and sufficient sample rate. In next section we will introduce how to measurement the ECG.

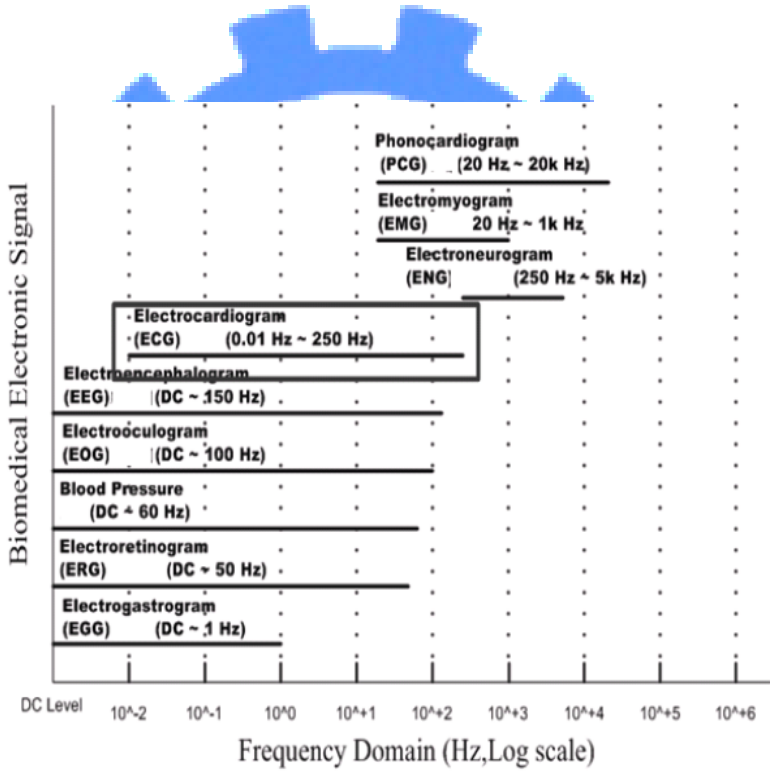

Figure 2-4 Frequency Distribution of Physiological Electronic Signal [Wang, 2008]

Table 2-1 Properties of Typical Bioelectric Signals [Chang, 2004]

Properties of typical bioelectric signals

Signal	Amplitude (mV)	Frequency range (Hz)
ECG	0.02 – 5.0	0.05 - 100
EEG (surface electrode)	0.0002 – 0.3	DC – 150
EEG (nail electrode)	0.01 – 50.0	DC – 150
EMG	0.1 – 5.0	DC – 10000
EGG	0.01 – 1.0	0.05 – 0.5
ERG	0 – 0.9	DC – 20
EOG	0.05 – 3.5	0.2 – 15
Nerve (external)	0.01 – 3.0	20 – 8000
Nerve (internal)	0.01 – 100	20 – 8000

2.2 ECG Measurement

As early as 1903, A Dutch physiologist named Willem Einthoven invented the first practical ECG. He proposed the Einthoven's Triangle [Einthoven's Triangle] described on **Figure 2-5**. This method is mainly corresponded to the heart electrical axis [NTHU]. This heart electrical axis presents primarily direction of electrical activity of heart. This direction always direct to the heart tip. The **Figure 2-5** expresses the three recording ways which were combined to Einthoven's Triangle as below:

- *The lead I about 0 degree records the process of depolarization from right arm to left arm.*
- *The lead II about 60 degrees records the process of depolarization from right arm to left leg.*
- *The lead III about 120 degrees records the process of depolarization from left arm to left leg.*

While the heart tip (or heart axis) parallel to one of them, and this lead will obtain the highest potential. Thus, according to section 2.1 described as upon, a series of activation of heart will be illustrated on this lead. So, we should be seen the activity situations of various position of heart. If any position of heart is broken, the ECG will

show it out.

According to Kirchhoff's Voltage, we can represent the relation between lead *I-III* as follow [李修誠, 2009]:

$$I - II + III = 0. \qquad (2.1)$$

In the **Figure 2-5** and **Figure 2-6**, the *aVR, aVF, and aVL* are the augmented limb leads.

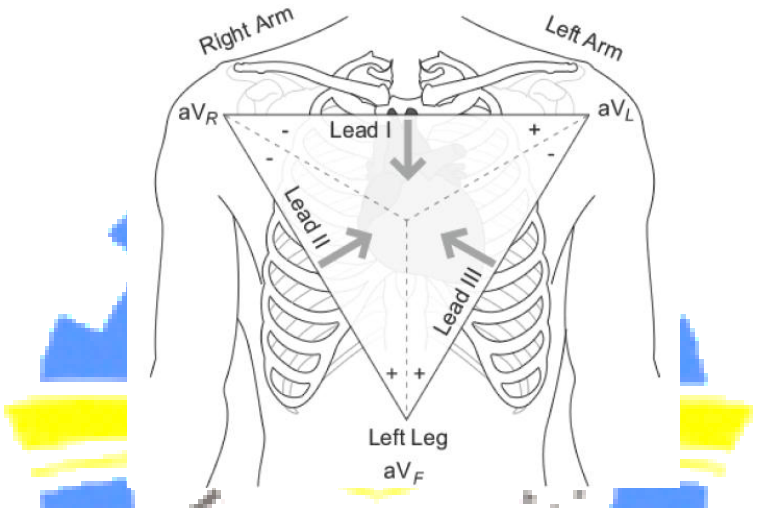

Figure 2-5 ECG Lead Positions of Limp [Wang, 2008]

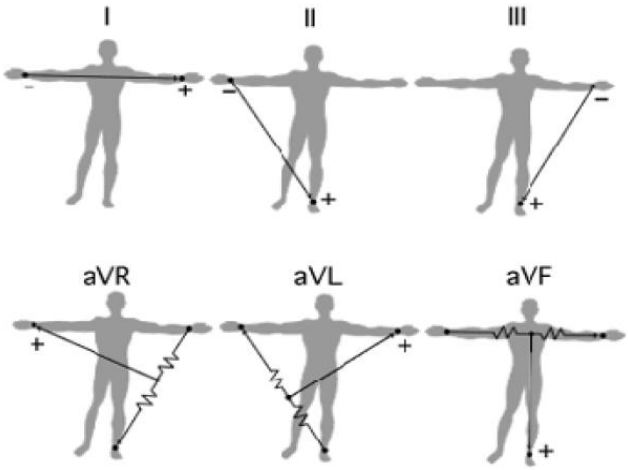

Figure 2-6 Bipolar Limb Derivations [Blioju, 2010]

If we using *V* to express each potential, then we can obtain [李修誠, 2009]:

$$I = V_{LA} - V_{RA} \qquad (2\text{-}2)$$

$$II = V_{LL} - V_{RA} \quad (2\text{-}3)$$

$$III = V_{LL} - V_{LA}. \quad (2\text{-}4)$$

According to **Figure 2-6**, we represent the relationship of *I, II, III, aVR, aVF, and aVL* as below:

$$aVR = -(Lead\ I + Lead\ II)\ /\ 2 \quad (2.5)$$

$$aVL = (Lead\ I - Lead\ III)\ /\ 2 \quad (2.6)$$

$$aVF = (Lead\ II + Lead\ III)\ /\ 2. \quad (2.7)$$

The lead *I, II, and III* describe the distinct pasting method of electrodes. The practical application will be introduced in chapter 3. Now, if we paste the electrodes correctly, we will obtain the actual ECG. According to **Table 2-1**, the small ECG signal is not enough to recognize. So, in next section, we will introduce the amplification of ECG signal.

2.3 ECG Amplifier

In **Table 2-1**, we know the ECG signal that is very tiny about 0.02-5mV. So, the amplifier must has the large amplification gain. The instrumentation amplifier (IA) consisted of several operation amplifier is a good choice because it has the high range of gain and the high Common Mode Rejection Ratio (*CMRR*). The CMRR is an index about capable of noise immunity of IA. The IA can amplify the gain from 0 to 1000. For the mV classes of ECG, this amplifier is enough to application, but the supply voltage need to regard. The process of catching the physiological signal is usually affected by common mode noise. This noise can't be reduced directly using the filter [Chang, 2004] because it exists with the heart signal. Therefore, we will introduce the CMRR function in next step.

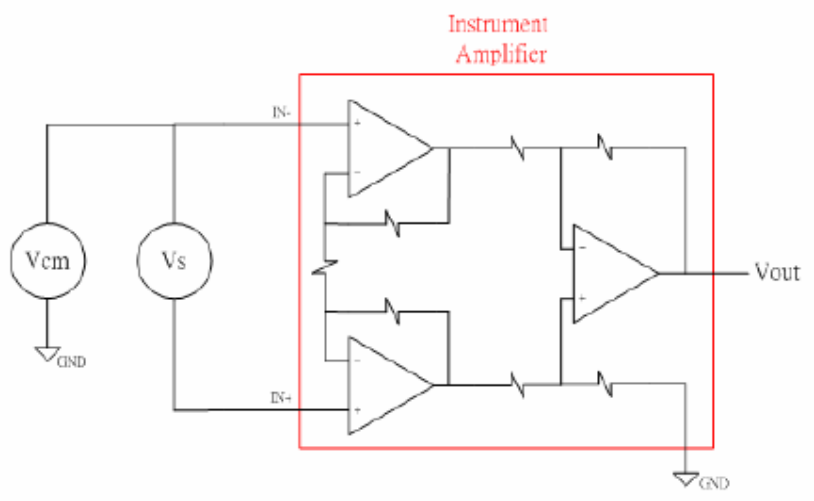

Figure 2-7 Differential Amplifier [Chang, 2004]

In the **Figure 2-7**, the V_{cm} is the common mode signal, and the V_s which signal we want to amplify that is the differential mode signal. Suppose the amplification gain of IA located in red frame is A, and then we can understand the signal amplified by IA is only V_s described as below:

$$V_{IN+} = V_{cm} + V_s$$

$$V_{IN-} = V_{cm}$$

$$V_{out} = A \times (V_{IN+} - V_{IN-}) \qquad (2.8)$$

$$V_{out} = A \times (V_{cm} + V_s - V_{cm})$$

$$V_{out} = A \times V_s.$$

In the Eq. (2.8), the V_{cm} is not be amplified, but this is an ideal condition. In the practical situation, the common mode noise is always presence. For solving this question, we refer an important index-value called *CMRR*. While the *CMRR* is high, the extent of signal that we want affected by common mode noise is small. Let the A_c be the amplification gain of V_{cm}, and then the A_d be the amplification gain of V_s. We can obtain the formula of *CMRR* as below:

$$CMRR(dB) = 20 \times log(\frac{A_d}{A_c}). \qquad (2.9)$$

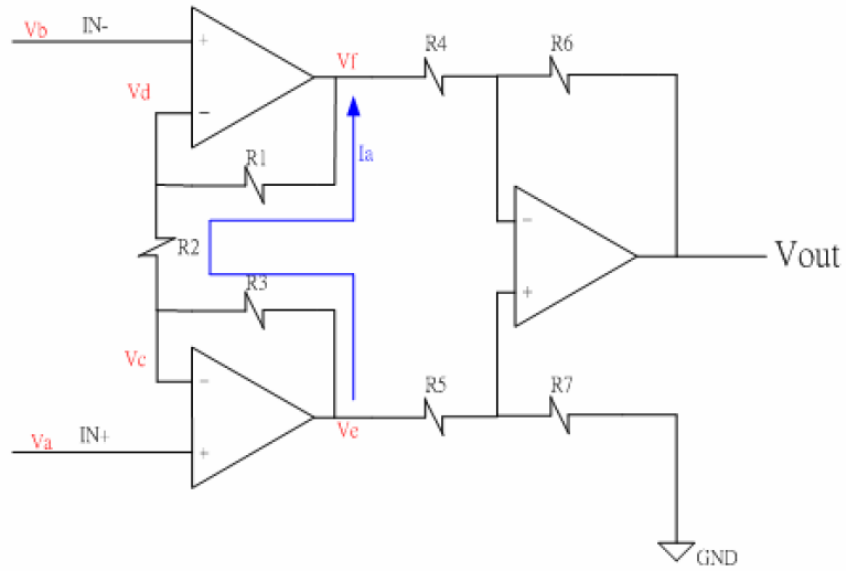

Figure 2-8 Instrumentation Amplifier [Chang, 2004]

According to **Figure 2-8**, due to the operation amplifier has the feature of virtual ground under the configuration of negative feedback. Thus, we can obtain:

$$V_a = V_c \quad , \qquad V_b = V_d$$

$$I_a = \frac{V_c - V_d}{R_2} = \frac{V_a - V_b}{R_2}$$

$$V_e - V_f = I_a \times (R_1 + R_2 + R_3) = \frac{V_a - V_b}{R_2} \times (R_1 + R_2 + R_3). \qquad (2.10)$$

We use the superposition theorem to calculate the contribution of V_e and V_f on V_{out}. First, let the V_f equal to 0, and calculate the contribution of V_e on V_{out} as follow:

$$V_{out} = V_e \times \frac{R_7}{R_5 + R_7} \times (1 + \frac{R_6}{R_4}). \qquad (2.11)$$

Afterward make the V_e equal to 0, and calculate the contribution of V_f on V_{out} as below:

$$V_{out} = V_f \times (-\frac{R_6}{R_4}). \qquad (2.12)$$

Thus, via combine the Eq. (2.11) and Eq. (2.12), we can obtain the contribution for V_{out} as follow:

$$V_{out} = V_e \times \frac{R_7}{R_5+R_7} \times \frac{R_4+R_6}{R_4} - V_f \times \frac{R_6}{R_4}. \quad (2.13)$$

Let the $R_4 = R_5$, $R_6 = R_7$, and Eq. (2.13) can be expressed as:

$$V_e \times \frac{R_6}{R_4} - V_f \times \frac{R_6}{R_4} = (V_e - V_f) \times \frac{R_6}{R_4}. \quad (2.14)$$

Afterward, substitute the Eq. (2.10) in Eq. (2.14), we can acquire:

$$V_{out} = \frac{V_a - V_b}{R_2} \times (R_1 + R_2 + R_3) \times \frac{R_6}{R_4}. \quad (2.15)$$

Finally, we can be obtained the amplification gain of IA by making the $R_1 = R_3$ described as follow:

$$V_{out} = (V_a - V_b) \times (1 + 2 \times \frac{R_1}{R_2}) \times \frac{R_6}{R_4}$$

$$A = \frac{V_{out}}{V_a - V_b} = (1 + 2 \times \frac{R_1}{R_2}) \times \frac{R_6}{R_4}. \quad (2.16)$$

At present, we finished the amplification of ECG signal, but the noise which is higher or particular (60 Hz power line) one still exists in the ECG signal. Thus, in the next section, we will explain these noises type.

2.4 ECG Noise

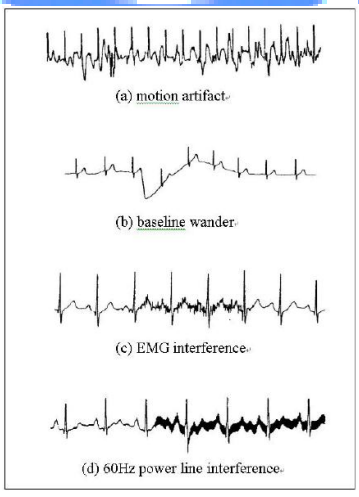

Figure 2-9 Distinct Interference Noise on the ECG [Luo, 2004]

The **Figure 2-9** shows the different noise on the ECG. The **Figure 2-9** (a)

illustrates the motion artifact noise. This noise is greatly hard to reduction. This type noise is caused by patient's movement [Lee, 2007]. While measuring the biopotential, the electrodes have the opportunity to move by patient motion. Thus, the electrodes glued on the skin will change the resistance. This influence causes the offset potential, and the baseline will be wandered described as **Figure 2-9** (b). Thus, our countermeasure for (a) and (b) are:

(1) Persuasion the patient who is as not to motion as possible.

(2) Using the clean electrodes to glue firmly on the skin.

(3) Employing the alcohol to clear the skin.

(4) Designing the better electrodes.

(5) Using our bracelet measuring way described in chapter 3.

The **Figure 2-9** (c) shows the Electromyographic (EMG) interference. This noise caused by the tremble of muscle of body, and that is a high frequency noise [Luo, 2004]. If we want to reduce this EMG interference, we can be referred these method described as bellow:

(1) Selecting the proper glued position of electrodes, and away the activity range of muscle as far as possible.

(2) Adding the low-pass filter on circuit for filtering the higher EMG signal.

The **Figure 2-9** (d) expresses the power-line interference (or 60 Hz). This noise caused by the magnetic field of transformer. By means of Maxwell-Faraday, when a varying magnetic field passes a conductor, this conductor will generate a potential. Thus, while the power-line carried the current generate a varying magnetic field and through a circuit loop, this loop will be produced an induction current. If this induction current enters the input of amplifier, the ECG will be affected by this current. Thus, our countermeasure is described as follow for reducing this noise:

(1) Employing the Notch filter to reduction this specific noise (60 Hz).

(2) Due to the induction current induced by magnetic field is proportional to the area of loop. Thus, we can interlace the conductor for reducing this area of loop described as in ***Figure 2-10****.*

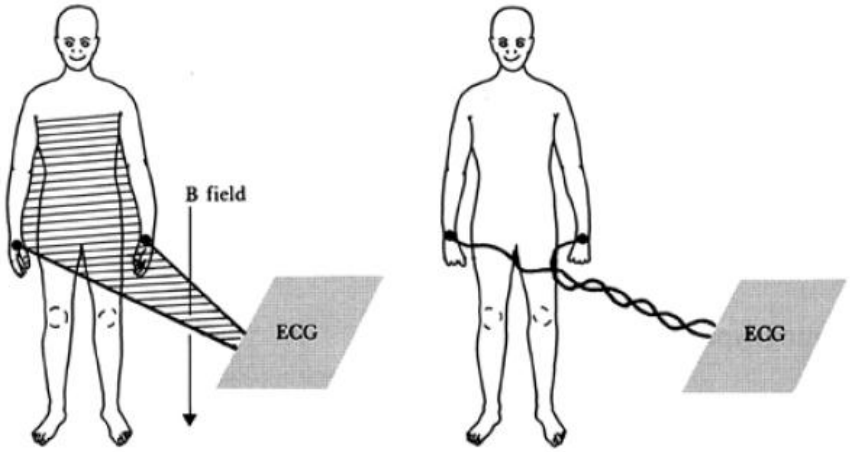

Figure 2-10 Interference of ECG by Magnetic Field of Power-Line [李修誠, 2009]

We finished introduction of these noises in this section. In next section, we will introduce the derivation of equations of Sallen-Kay filter for design this filter.

2.5 Sallen-Kay Low-Pass Filter

Usually, we hope to possess the low-pass filter of high Q-factor. The typical two order low-pass filter described as **Figure 2-11** is restricted by its low Q-factor which is close to 0.5 or smaller than 0.5. Thus, via controlling the number of feedback of amplifier, we can implement the high Q-factor active filter.

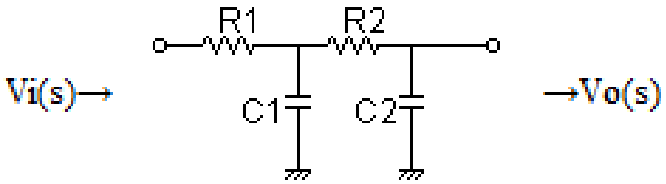

Figure 2-11 Typical Two-Order of Low-Pass Filter [OKAWA, 2008]

Under the **Figure 2-12**, when the V_{in} is a low-frequency, *C1* and *C2* are open.

The V_{in} pass through the filter to V_{out} completely. While the V_{in} is a high-frequency, *C1* and *C2* change to short. Thus, all the signal of V_{in} pass through the short *C2* to ground end. The V_{out} can't export the V_{in} signal. Hence, we know this filter is a two order active low-pass filter.

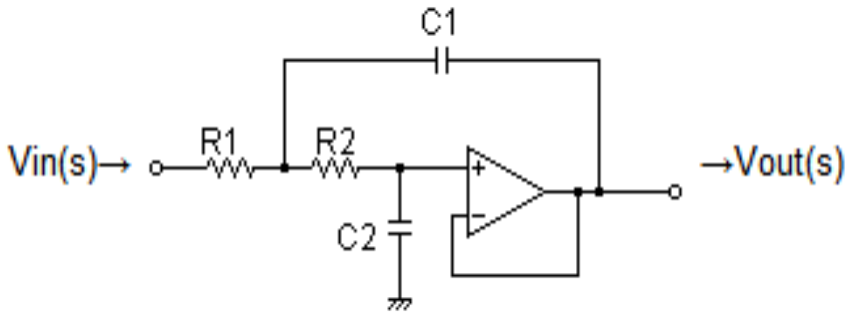

Figure 2-12 Unity Gain Sallen-Kay Low-Pass Filter [OKAWA, 2008]

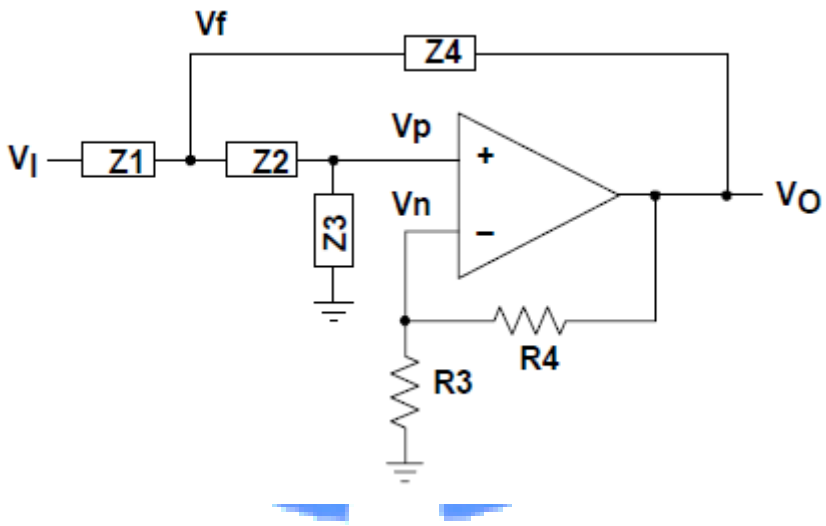

Figure 2-13 Generalized Sallen-Kay Circuit [Sallen-Key, 1999]

The **Figure 2-13** is a generalized Sallen-Kay Circuit. In the light of Kirchhoff's law (KCL), the current equation of node *Vf* can be expressed as:

$$\frac{V_I - Vf}{Z1} = \frac{Vf - Vp}{Z2} + \frac{Vf - V_o}{Z4}$$

$$\frac{V_I}{Z1} + \frac{Vp}{Z2} + \frac{Vo}{Z4} = \frac{Vf}{Z1} + \frac{Vf}{Z2} + \frac{Vf}{Z4}$$

$$Vf \times \left(\frac{1}{Z1} + \frac{1}{Z2} + \frac{1}{Z4}\right) = V_I \times \frac{1}{Z1} + Vp \times \frac{1}{Z2} + V_o \times \frac{1}{Z4}. \qquad (2.17)$$

The *Vp* can be described as:

$$\frac{Vf - Vp}{Z2} = \frac{Vp}{Z3}$$

$$Vp \times \left(\frac{1}{Z2} + \frac{1}{Z3}\right) = Vf \times \frac{1}{Z2}$$

$$Vf = Vp \times \left(1 + \frac{Z2}{Z3}\right). \quad (2.18)$$

Let the Eq. (2.18) substitute in Eq. (2.17). We will obtain the Eq. (2.19) as below [Sallen-Key, 1999]:

$$Vp \times \left(1 + \frac{Z2}{Z3}\right) \times \left(\frac{1}{Z1} + \frac{1}{Z2} + \frac{1}{Z4}\right) = V_I \times \frac{1}{Z1} + Vp \times \frac{1}{Z2} + V_O \times \frac{1}{Z4}$$

$$Vp\left(\frac{Z2 + Z3}{Z3}\right)\left(\frac{Z2Z4 + Z1Z4 + Z1Z2}{Z1Z2Z4}\right) - Vp \times \frac{1}{Z2} = V_I \times \frac{1}{Z1} + V_O \times \frac{1}{Z4}$$

$$Vp\left(\frac{Z2Z2Z4 + Z1Z2Z4 + Z1Z2Z2 + Z2Z3Z4 + Z1Z3Z4 + Z1Z2Z3}{Z1Z2Z3Z4}\right) - Vp \times \frac{1}{Z2}$$

$$= V_I \times \frac{1}{Z1} + V_O \times \frac{1}{Z4}$$

$$Vp\left(\frac{Z2Z2Z4 + Z1Z2Z4 + Z1Z2Z2 + Z2Z3Z4 + Z1Z2Z3}{Z1Z2Z3Z4}\right) = V_I \times \frac{1}{Z1} + V_O \times \frac{1}{Z4}$$

$$+V_O\left(\frac{Z1Z2Z3}{Z2Z2Z4+Z1Z2Z4+Z1Z2Z2+Z2Z3Z4+Z1Z2Z3}\right). \quad (2.19)$$

Hence, according to the KCL, we can know the current equation of node *Vn* as follow:

$$Vn = V_O \times \frac{R3}{R3+R4}. \quad (2.20)$$

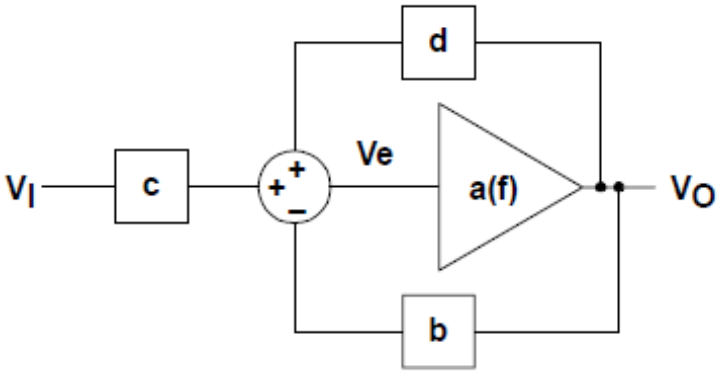

Figure 2-14 Gain-Block Diagram of the Generalized Sallen-Kay Filter [Chang, 2004]

The **Figure 2-14** is the gain-block diagram of Sallen-Kay filter. The value in this diagram can be explained as below:

a(f) is the open loop gain of operation amplifier

$$b = \frac{R3}{R3 + R4}$$

$$c = \left(\frac{Z2Z3Z4}{Z2Z2Z4 + Z1Z2Z4 + Z1Z2Z2 + Z2Z3Z4 + Z1Z2Z3}\right)$$

$$d = \left(\frac{Z1Z2Z3}{Z2Z2Z4 + Z1Z2Z4 + Z1Z2Z2 + Z2Z3Z4 + Z1Z2Z3}\right)$$

$$Ve = Vp - Vn.$$

From the upon gain-block diagram, we can obtain:

$$V_O = a(f) \times Ve \qquad (2.21)$$

$$Ve = c \times V_I + d \times V_O + b \times V_O. \qquad (2.22)$$

Combining Eq. (2.21) and Eq. (2.22) can be acquired as follow:

$$V_O = a(f) \cdot (c \cdot V_I \cdot d \cdot V_O - b \cdot V_O) = a(f) \cdot c \cdot V_I \cdot a(f) \cdot d \cdot V_O - a(f) \cdot b \cdot V_O$$

$$V_O - a(f) \cdot d \cdot V_O + a(f) \cdot b \cdot V_O = a(f) \cdot c \cdot V_I$$

$$V_O[1 - a(f) \cdot d + a(f) \cdot b] = a(f) \cdot c \cdot V_I$$

$$\frac{V_O}{V_I} = \frac{a(f) \cdot c}{1 - a(f) \cdot d + a(f) \cdot b}$$

$$\frac{V_O}{V_I} = \frac{c}{\frac{1}{a(f)} - d + b} = \frac{c}{b} \times \left(\frac{1}{1 + \frac{1}{a(f)} - \frac{d}{b}}\right). \qquad (2.23)$$

The Eq. (2.23) is the transform function for Sallen-Kay filter. Due to the open-loop gain $a(f) \cong \infty$ in ideal operation amplifier, that is $\frac{1}{a(f)} \cong 0$. Thus, Eq. (2.23) can be changed to:

$$\frac{V_O}{V_I} = \frac{c}{b} \times \frac{1}{1 - \frac{d}{b}}. \qquad (2.24)$$

Making $\frac{1}{b} = K, c = \frac{N1}{D}, d = \frac{N2}{D}$ substituted in Eq. (2.24):

$$\frac{V_O}{V_I} = K \cdot \frac{N1}{D} \times \frac{1}{1-K\cdot\frac{N2}{D}} = \frac{K}{\frac{D}{N1}-K\cdot\frac{N2}{N1}}. \quad (2.25)$$

Therefore, we can be further represented as:

$$K = \frac{1}{b} = \frac{R3+R4}{R3}$$

$$D = Z2Z2Z4 + Z1Z2Z4 + Z1Z2Z2 + Z2Z3Z4 + Z1Z2Z3$$

$$N1 = Z2Z3Z4$$

$$N2 = Z1Z2Z3. \quad (2.26)$$

Substituting the Eq. (2.26) in Eq. (2.25) can be acquired as below:

$$\frac{V_O}{V_I} = \frac{K}{\frac{Z2Z2Z4+Z1Z2Z4+Z1Z2Z2+Z2Z3Z4+Z1Z2Z3}{Z2Z3Z4} - K\cdot\frac{Z1Z2Z3}{Z2Z3Z4}}$$

$$\frac{V_O}{V_I} = \frac{K}{\frac{Z2}{Z3}+\frac{Z1}{Z3}+\frac{Z1Z2}{Z3Z4}+\frac{Z1}{Z4}+1-K\cdot\frac{Z1}{Z4}}. \quad (2.27)$$

Due to the open-loop gain of operation amplification can be supposed to infinite. Thus, the transform function of Sallen-Kay filter can be simplified to the ideal situation described as follow:

$$\frac{V_O}{V_I} = \frac{K}{\frac{Z1Z2}{Z3Z4}+\frac{Z1}{Z3}+\frac{Z2}{Z3}+1+\frac{Z1}{Z4}\cdot(1-K)}. \quad (2.28)$$

Because the noises of ECG that we care are high frequency noise described at section 2.4, so we need a low-pass filter to leach the frequency higher than 100 Hz. In the next section, we will design the low-pass filter by using the ideal transform function expressed as Eq. (2.28).

2.6 Design the Filter

In this section, we will design the Sallen-Kay filter. The Eq. (2.29) presents a standard two-order low-pass filter.

$$H_{LP} = \frac{K}{-\left(\frac{f}{fc}\right)^2 + j\frac{f}{Q\cdot fc}+1}. \quad (2.29)$$

In Eq. (2.29), the *fc* is corner frequency, and *Q* is quality factor. The filter enters the

different frequency, and presents its results described as follow:

$$\begin{cases} Supposing\ the\ f \ll fc, & H_{LP} = K \\ Supposing\ the\ f = fc, & H_{LP} = -JQK \\ Supposing\ the\ f \gg fc, & H_{LP} = -K \cdot \left(\frac{fc}{f}\right)^2 . \end{cases}$$

If $H_{LP} = K$, the gain factor K will multi with signal which is entered in filter. Afterward, if $H_{LP} = -JQK$, the signal will be increased by quality factor Q. Finally, if $f >> fc$, the signal will be weaken to square times of frequency ratio. Thus, the Eq. (2.29) describes a two-order low-pass filter.

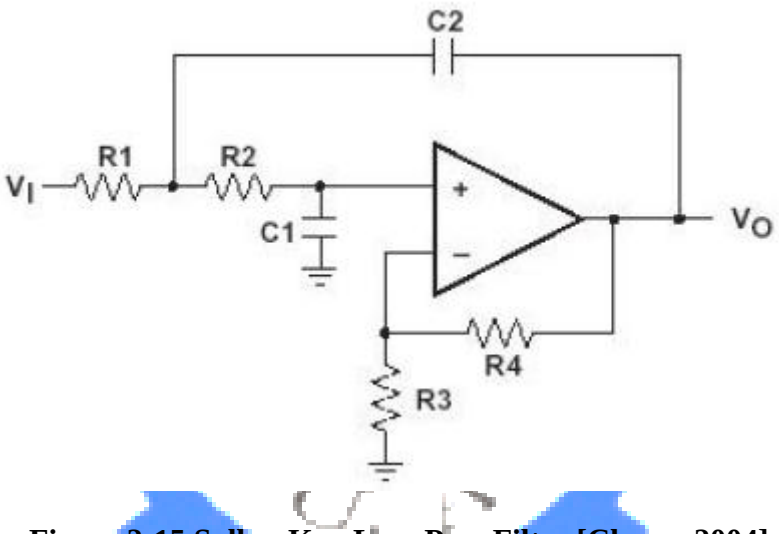

Figure 2-15 Sallen-Kay Low-Pass Filter [Chang, 2004]

The **Figure 2-15** is Sallen-Kay low-pass filter. According to **Figure 2-13**, we obtain:

$$Z1 = R1$$

$$Z2 = R2$$

$$Z3 = \frac{1}{SC1}$$

$$Z4 = \frac{1}{SC2}$$

$$K = \frac{R3+R4}{R3} = 1 + \frac{R4}{R3}. \qquad (2.30)$$

We substitute Eq. (2.30) in Eq. (2.28), and represent as:

$$\frac{V_O}{V_I} = \frac{K}{S^2(R1R2C1C2)+S\left(R1C1+R2C1+R1C2(1-K)\right)+1}. \qquad (2.31)$$

where

$S = j2\pi f$

$j = \sqrt{-1}$.

Comparing Eq. (2.31) with Eq. (2.29) can obtain:

$$fc = f_L = \frac{1}{2\pi\sqrt{R1R2C1C2}} \quad (2.32)$$

and

$$Q = \frac{\sqrt{R1R2C1C2}}{R1C1+R2C1+R1C2(1-K)} \quad (2.33)$$

where the f_L is the cut-off frequency of low-pass filter.

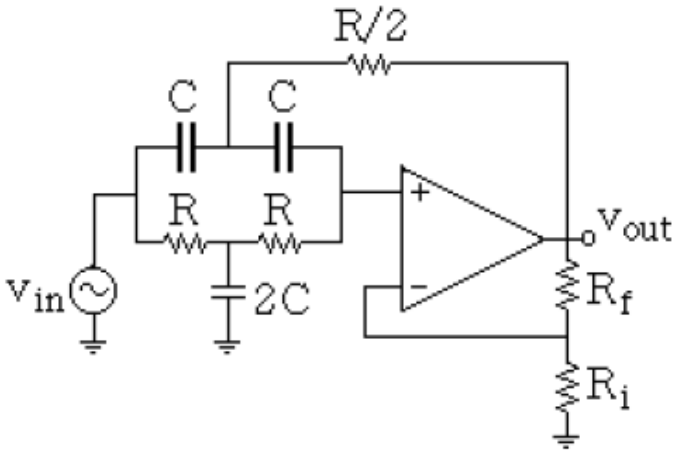

Figure 2-16 Sallen-Kay Second-Order Notch Filter [葉倍宏, 2010]

Although the noise which is higher one is filtered by upon method, but the power-line noise can't reduction by it. The **Figure 2-16** Notch filter is a common method for filtering this specific noise 60 Hz. In the low frequency, the capacitance is open. Thus, the input signal enters from inverting input. The voltage gain is:

$$A_{cl} = 1 + \frac{R_f}{R_i} \quad (2.34)$$

where the A_{cl} is close-loop gain.

In the high frequency, the capacitance is short. Thus, the input signal enters from inverting input, too. Sum of upon, both the low and high frequency have the output.

Hence, we can be known this filter is a band-stop filter. This filter's central frequency f_o and quality factor Q can be described as:

$$f_O = \frac{1}{2\pi RC} \tag{2.35}$$

and

$$Q = \frac{0.5}{2 - A_{cl}} \tag{2.36}$$

So far, we finished the filter design, and next section we will introduce the system configuration.

CHAPTER 3

SYSTEM CONFIGURATION

This section will introduce the throughout system configuration. The system configuration is described in **Figure 3-1**. The HARDWARE expresses the signal acquisition using Einthoven's Triangle, and signal processing employing the amplifier and filter. The SOFTWARE describes the QRS detection shown the ECG features wave; the R-R detection shown the R wave capturing and R-R interval detection; the HRV detection shown the detection of heart rate variability.

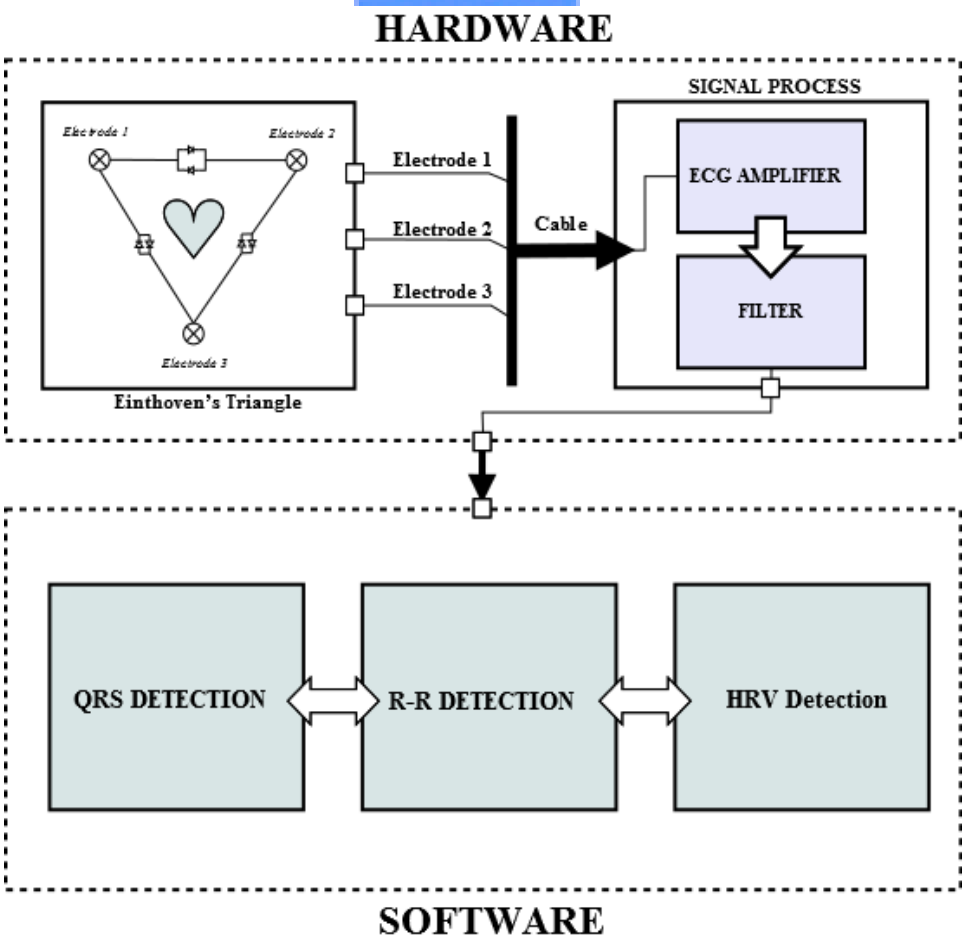

Figure 3-1 System Configuration

Soon afterwards, we will discuss the each part of system configuration step by step. Introduction sequence is:

- *The section 3.1 illustrates the measurement configuration of Einthoven's Triangle.*
- *The section 3.2 illustrates the practical application of signal optimization.*
- *The section 3.3 demonstrates the system configuration of software.*
- *The section 3.4 demonstrates the process of QRS detection.*
- *The section 3.5 demonstrates the process of R-R interval detection.*
- *The section 3.6 demonstrates the process of HRV detection.*
- *The section 3.7 shown the extended application on MSP430F5438 EVM [T. I., 2010].*

3.1 Configuration of Einthoven's Triangle

In the chapter 2, we already discussed the Einthoven's Triangle. Before measuring the ECG signal, we introduce the ECG sensors first. In this paper, we use the 10 NT coins as the sensors shown as **Figure 3-2**.

Figure 3-2 Coin Sensors

In view of the traditional electrode is easily fall into disuse because this type electrode is using an adhesive area which is disposable feature to fix them properly to the skin [Segura-Juarez et al., 2004]. Thus, using this kind of electrode maybe two or three times later, and the electrode will become to unable one. In normally, this electrode is not cheap which is sold from thirty to seventy at auction site or physical

store. For long-term using on experiment, the expenditure is too much for bearing. Fortunately, we find this method that is using the coin as the sensor [Rusu et al., 2008]. Using the coin as sensor, we can re-use it repeatedly, freely, and indefinitely. Before employing it, we just utilize the 3M tape to fix it on body.

Consequently, we paste the coin electrodes on body for recording the process of depolarization of heart. In line with the **Figure 2-5** and **Figure 2-6**, we can know the way of stick. The different position of glue will shows the distinct depolarization place on heart illustrated as **Figure 2-3**. The measuring result of my heart signal is shown as below:

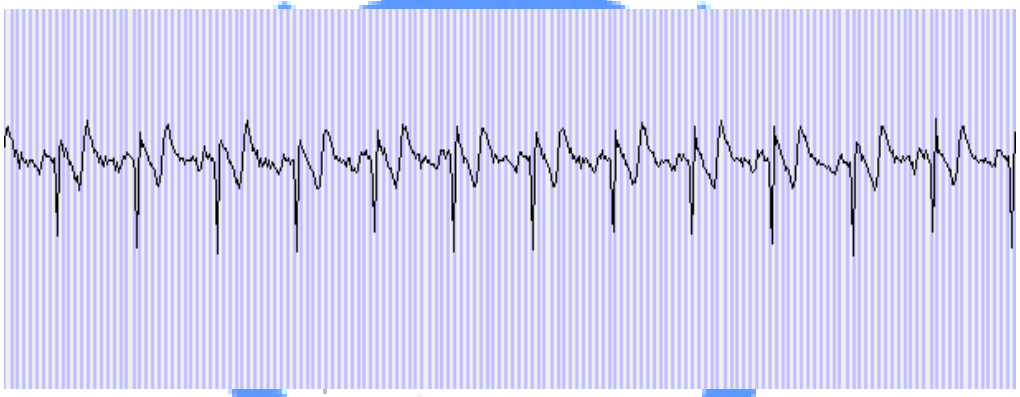

Figure 3-3 Reverse ECG of Lead I

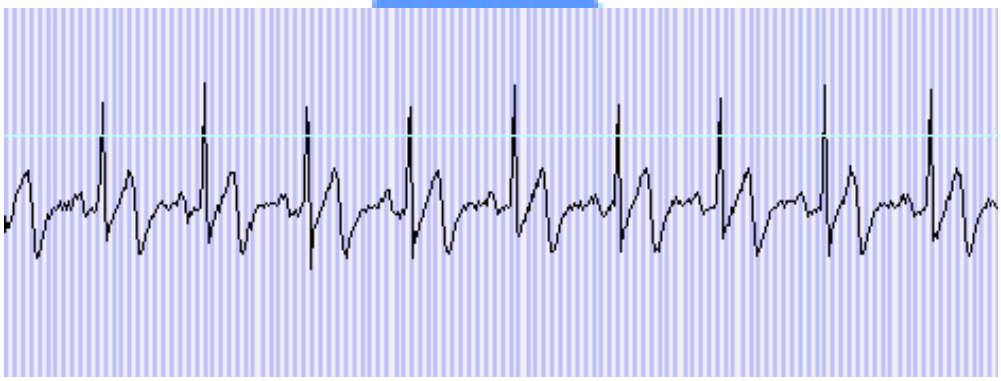

Figure 3-4 ECG of Adjusted Lead I

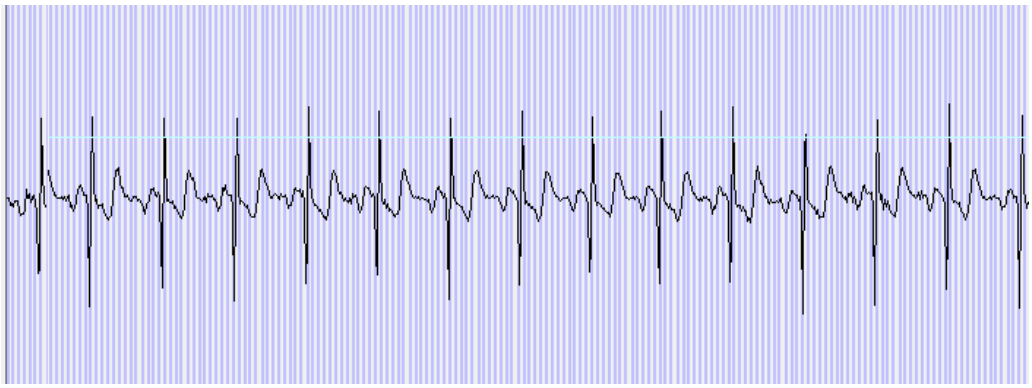

Figure 3-5 ECG of Lead II

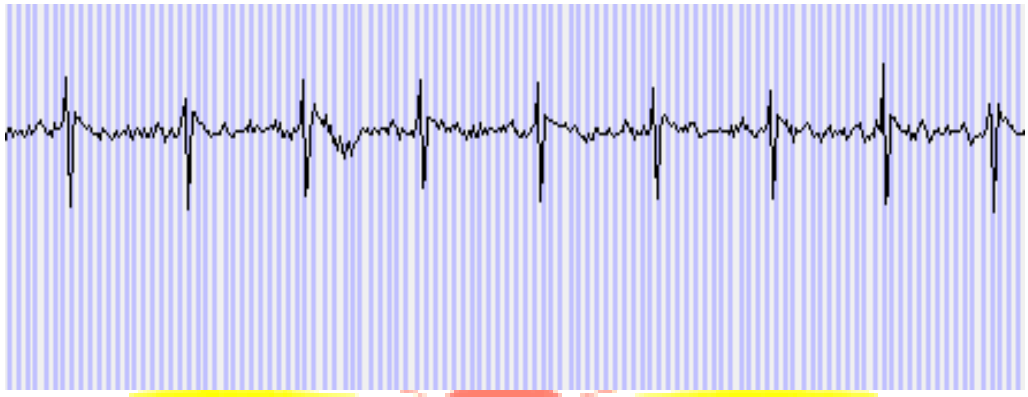

Figure 3-6 ECG of Lead III

In the **Figure 3-3**, we obtain the reverse QRS wave because our display system is inverse between positive and negative. On the basis of chapter 2, we know the lead recorded the process of depolarization of heart, and that mean about depolarization is recording the signal from negative to positive potential. Hence, exchanging the positive and negative electrode is not enough to affect the measurement result. So, we represent the ECG of lead I on **Figure 3-4** which is a normal ECG signal. In **Figure 3-5** and **Figure 3-6**, we show the lead II and lead III signal respectively. Comparing upon **Figure 3-3** – **Figure 3-6** with **Figure 3-7** – **Figure 3-8** describes as follow:

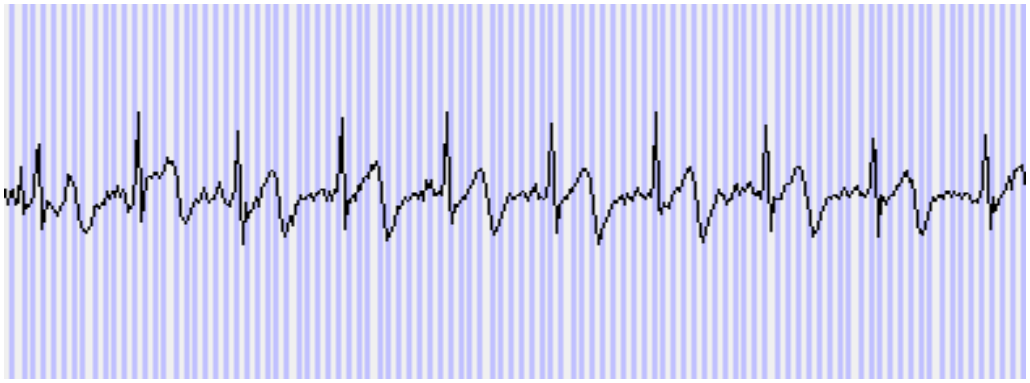

Figure 3-7 ECG of Lead I of Schoolmate A

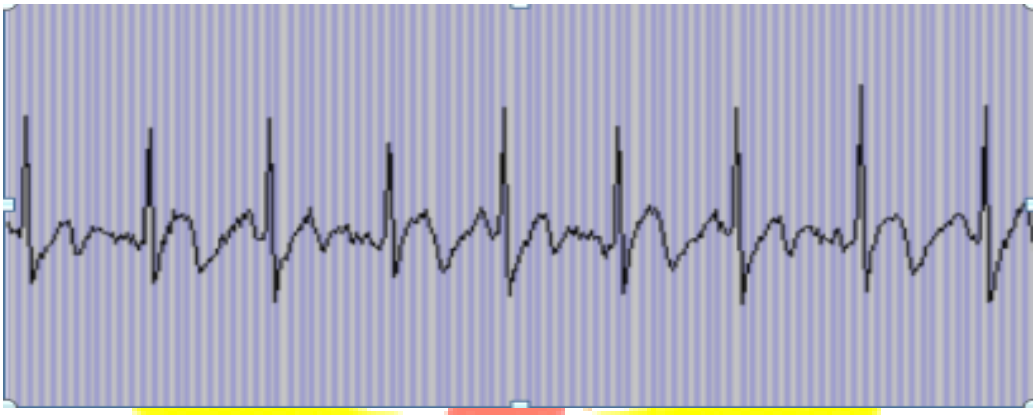

Figure 3-8 ECG of Lead II of Schoolmate A

We shall find that the **Figure 3-7** and **Figure 3-8** are very closely, and distinct with previous is only the lead I. That is because the heart tip is located from -30 degrees to 90 degrees in the normal situation shown as **Figure 3-9**. In **Figure 3-9**, the green line is iso-electric lead, and the arrow is heart tip position. Further, we can realize the heart tip is always located among the lead I and lead II in a health adult.

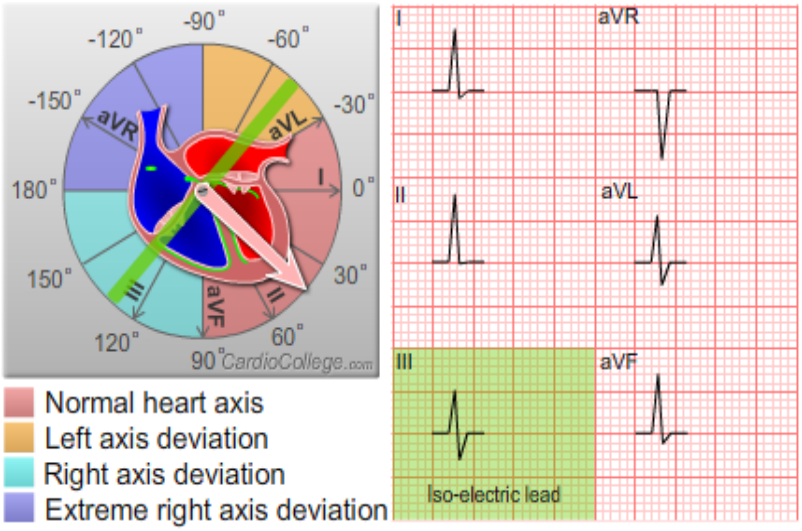

Figure 3-9 The Comparison Diagram of Heart Tip and ECG [Medical-eLearning, 2012]

Because the most adult's heart tip always direct to the 50 degrees. Hence, we can simplify the three leads to one lead II. For acquiring the maximum heart signal, we alter the lead II to:

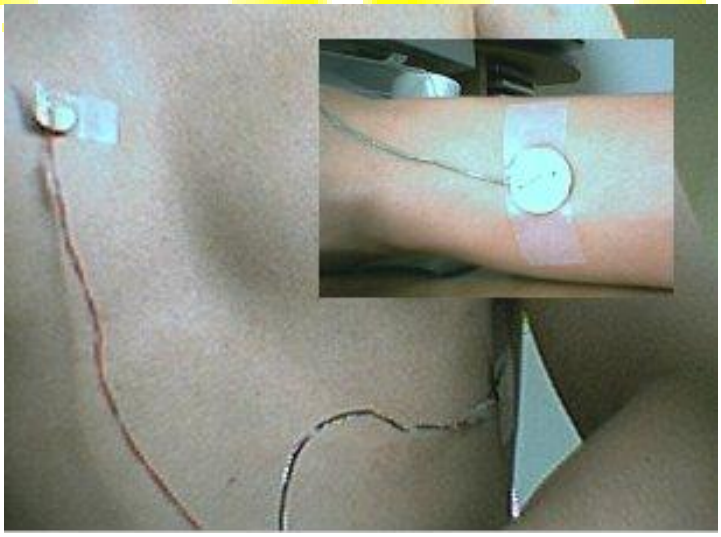

Figure 3-10 Simplified Lead II

The simplified lead II is fixed the electrodes on chest for acquiring the largest signal. In the **Figure 3-10**, the green cable is body lead which can help the body became to the loop for increasing the signal. By the way, if using the standard triangle lead, we can employ the relation between leads to find the heart tip position or the ill position

of heart. Now, we finished the triangle lead introduction, and next section we will introduce the signal optimization.

3.2 Practical Application of Signal Optimization

This section we will introduce the signal optimization further. According to Eq. (2.16), the amplification gain of **Figure 3-11** is:

$$A = \left(1 + 2 \times \frac{R1}{R2}\right) \times \frac{R6}{R4} = \left(1 + 2 \times \frac{100k}{1k}\right) \times \frac{100k}{100k} \cong 200.$$

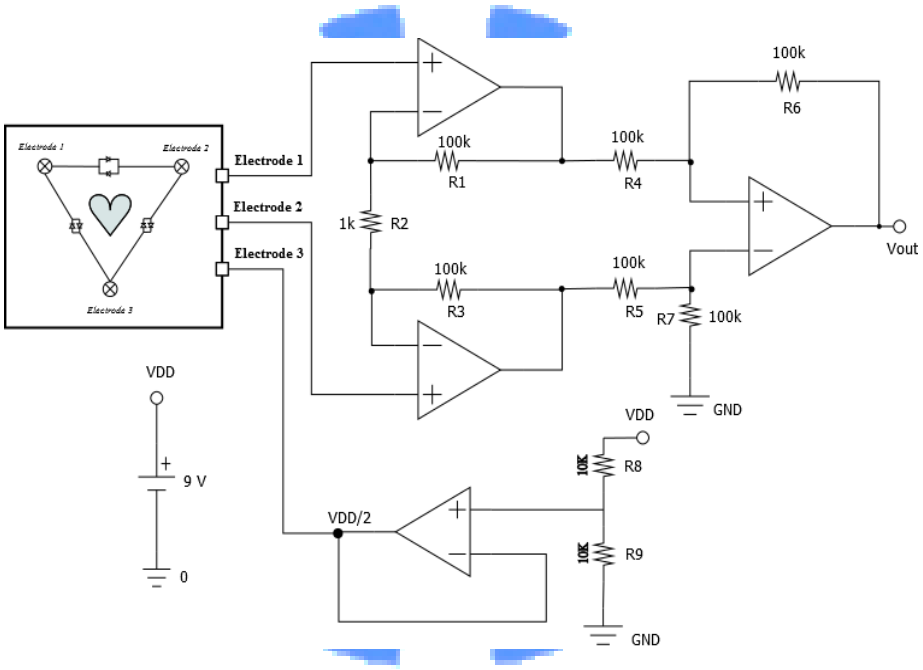

Figure 3-11 Diagram of Instrument Amplifier

So, in the light of **Table 2-1**, the 5 mV ECG potential can become to 1 V described as **Figure 3-12**.

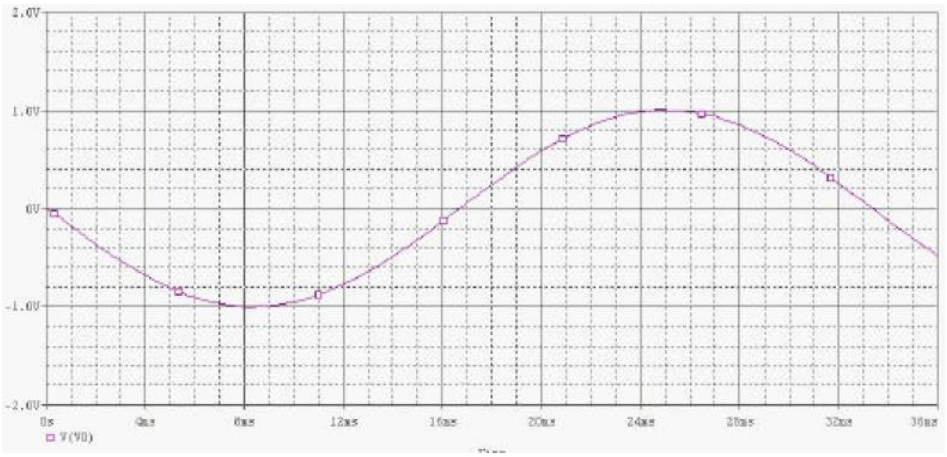

Figure 3-12 Simulation Diagram of IA in Time-Domain

We will reduce the noise of amplified signal. On the basis of **Figure 2-15**, if the cut-off frequency that we acquiring is 50 Hz, we make the each component values described as **Figure 3-13**.

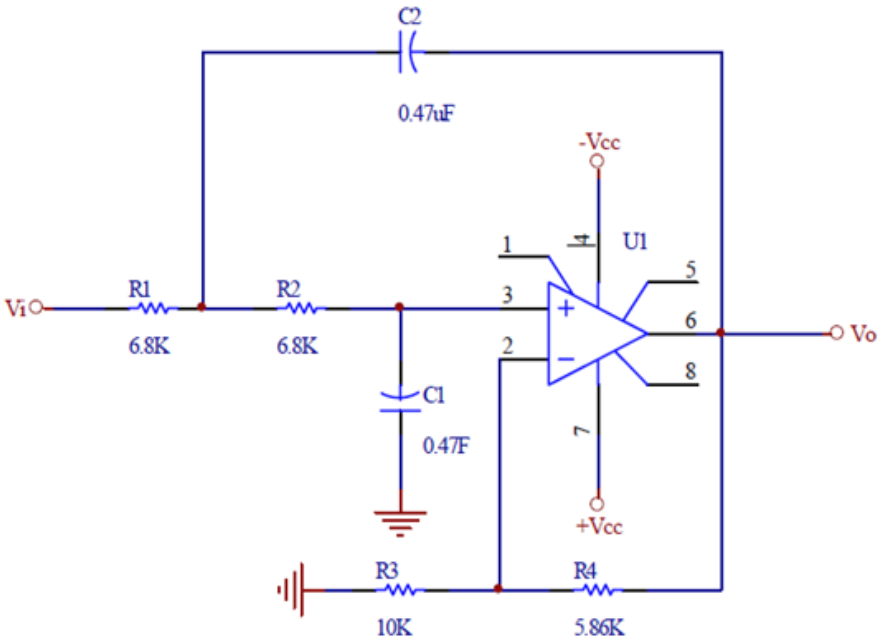

Figure 3-13 Circuit of Sallen-Kay Low-Pass Filter

The cut-off frequency of this filter will be:

$$fc = f_L = \frac{1}{2\pi \cdot \sqrt{6.8k \times 6.8k \times 0.47u \times 0.47u}} \cong 50\ Hz.$$

Thus, if the signal is over the 50 Hz, that will be reduced, and the extent of reduction can be described as **Table 3-1**. Our two-order filter is decay rate of -40 dB, and its

mean is the cut-off frequency is at decline of 3dB.

Table 3-1 Feature of Each Order of Low-Pass Filter

階 (Order)	衰減率 dB/decade	1 級 極點	DF	R_f/R_i	2 級 極點	DF	R_f/R_i	3 級 極點	DF	R_f/R_i
1	-20	1	選項							
2	-40	2	1.414	0.586						
3	-60	2	1	1	1	1	1			
4	-80	2	1.848	0.152	2	0.765	1.235			
5	-100	2	1	1	2	1.618	0.382	1	0.618	1.382
6	-120	2	1.932	0.068	2	1.414	0.586	2	0.518	1.482

Each 10 times cut-off frequency will decay 40 dB, and that frequency response is shown as **Figure 3-14**:

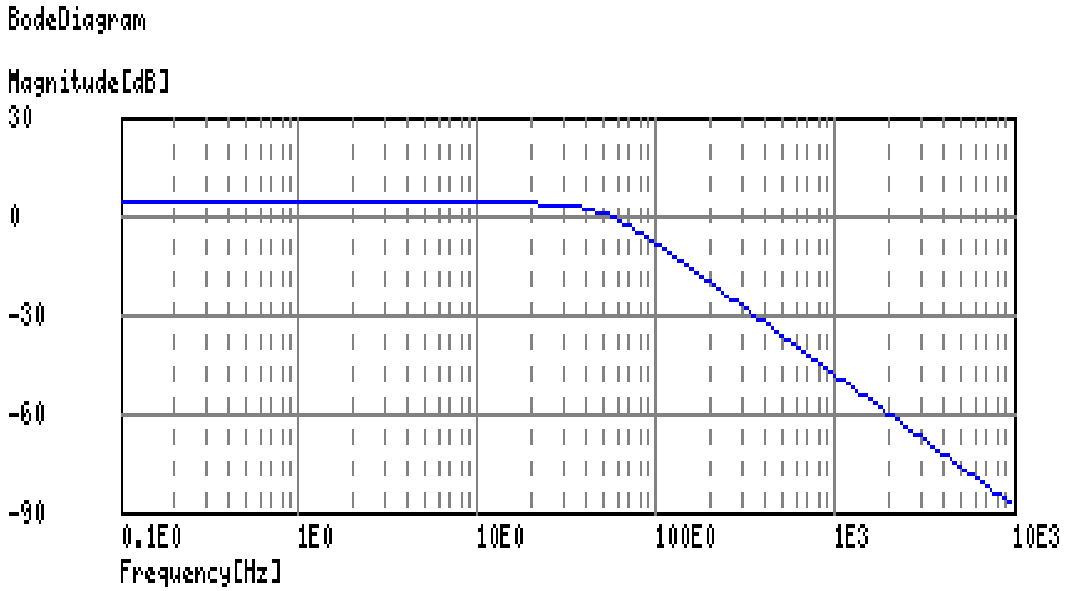

Figure 3-14 Frequency Response of Sallen-Kay Low-Pass Filter

The higher noise was already reduced by filter, and next step we need to remove the specific noise of 60 Hz. Hence, we will utilize the notch filter to remove it.

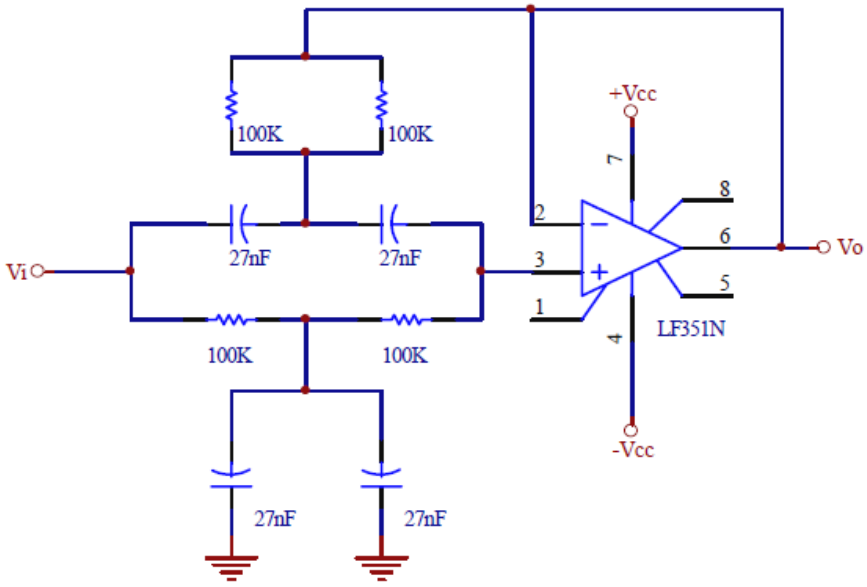

Figure 3-15 Circuit of Notch Filter

The **Figure 3-15** express the 60 Hz filter, and its frequency response is shown as **Figure 3-16**.

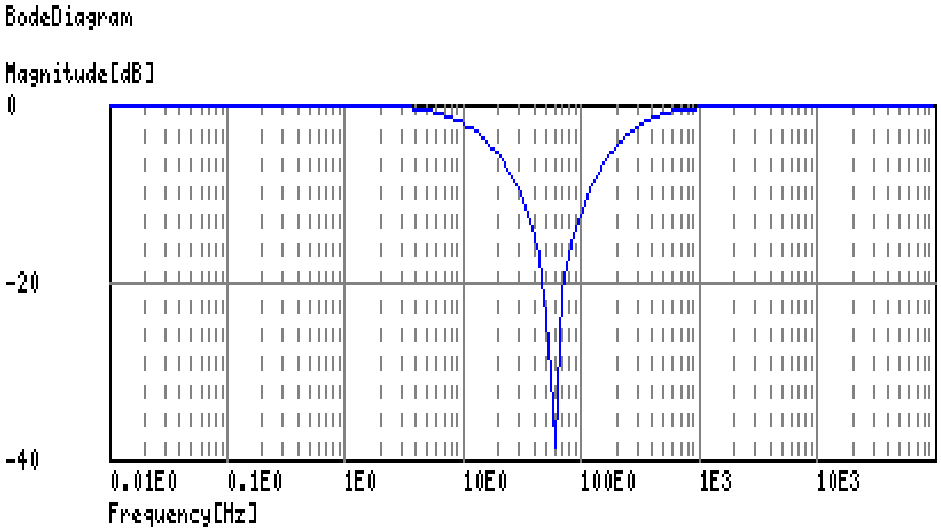

Figure 3-16 Frequency Response of Notch Filter

3.3 System Configuration of Software

In this section, we will discuss about the configuration of software, and its flow chart is described as **Figure 3-17**. Our configuration of software is built by using the

Visual Basic 6.0 (VB6). Using the VB6 to construction the part of software is usually very hard because the Application Programming Interface (API) [API] function which is utilized for quoting the Windows functions for extending the capability of VB6 is sealed by Microsoft Company. You cannot to know how it works inside these functions. Hence, you need to sufficient understand its usage first.

Due to our system transmission the ECG signal from Hardware to Software is using the microphone port of PC. Therefore, we must utilize the API function, if we want to utilize the sound card plugged into the computer. The sound card can convert the analog signal to digital signal for application further [Sound Card].

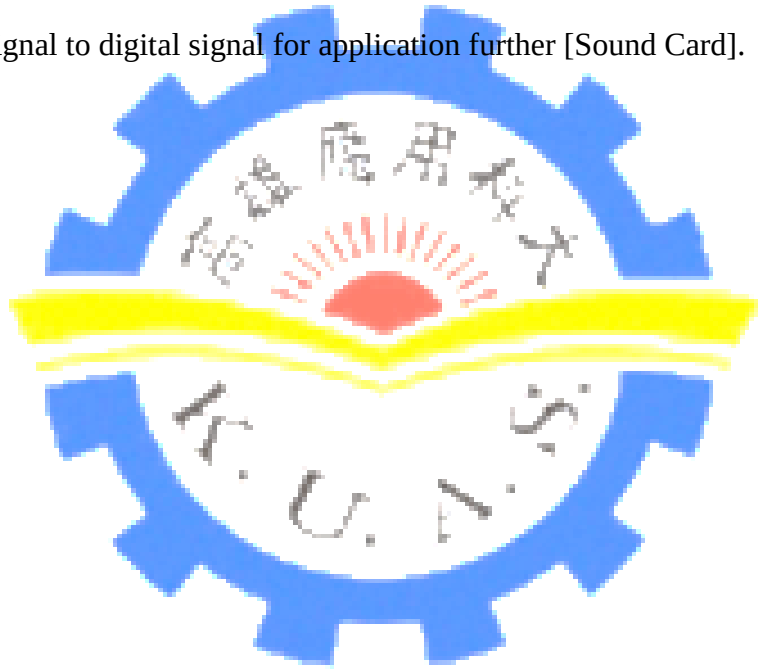

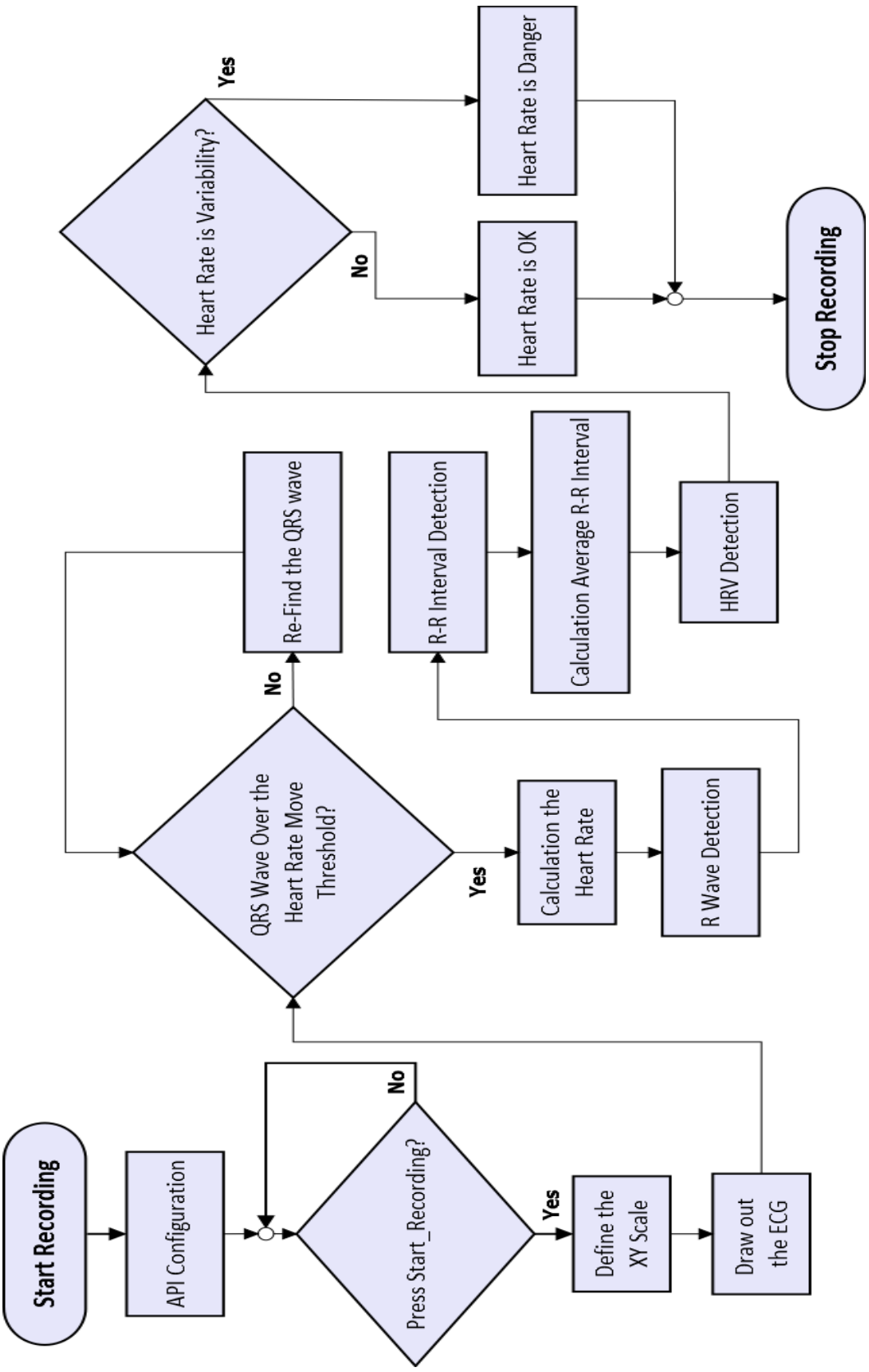

Figure 3-17 Configuration of Software Flow Chart

We are well known the voice which is a kind of energy transmission. The voice converted the analog signal to potential signal via the microphone [Microphone], and that is played by using the sound card on the person computer. Thus, the measured potential from heart can utilize the same way to convert it. So, we employing the TRS connect (tip, ring, sleeve) [TRS Connector] to connect with PC described as **Figure 3-18**.

Figure 3-18 Employing the TRS to Connect With PC

The TRS structure is shown as:

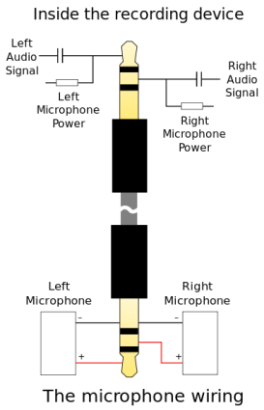

Figure 3-19 TRS 3.5 mm Stereo Plug [TRS Connector]

In the VB6, if you want to use the specific perform on PC, you need to declare

the corresponding API function. Afterward, the specific perform that we want to utilize is sound card plugged in PC. The API function which is dealt the audio described as follow:

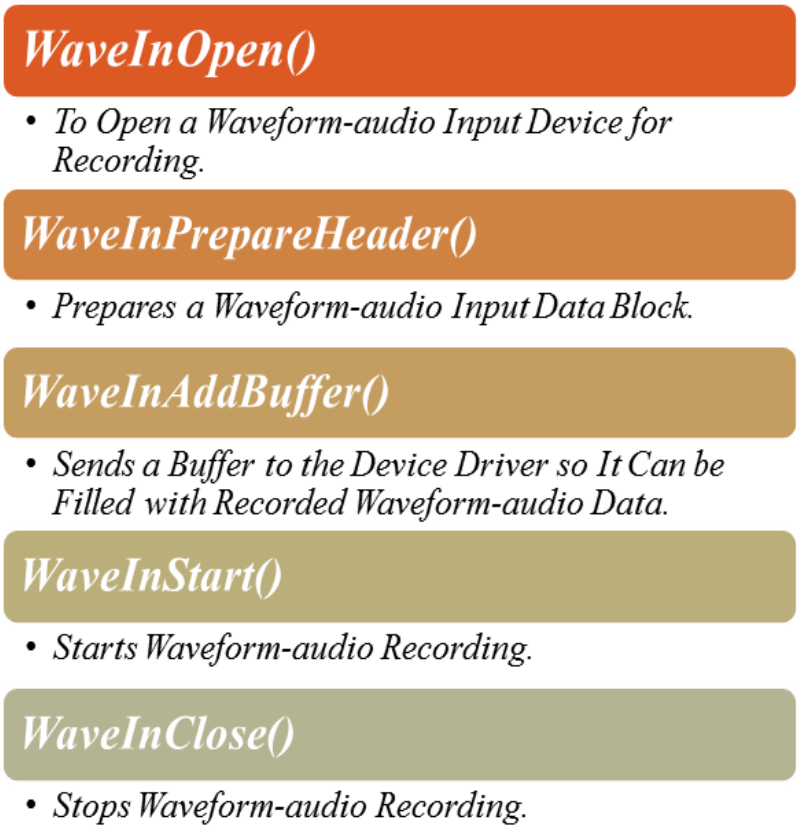

Figure 3-20 API Function of Low-Level Wave Audio

The **Figure 3-20** is a specialization audio waveform of API function which is called Low-Level Wave Audio (LLWA) [Group, 1998]. Employing a API function to record the analog signal on sound card has a lot procedure [MSDN]. Therefore, we just utilize the so-called Low-Level Wave Audio to simplify the procedure. In **Figure 3-20**, we introduce the rough usage for each LLWA functions.

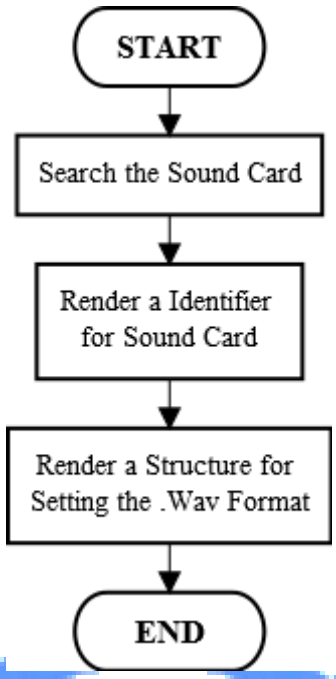

Figure 3-21 Function of WaveInOpen

The **Figure 3-21** shows the process of WaveInOpen function. The .Wav is so-called Waveform Audio File Format (WAVE) [Waveform Audio File Format]. This format is proposed by Microsoft and IBM. It is an audio coded format which is using the Resource Interchange File Format (RIFF) [Wilson, 2003] to record the audio. Afterward, each part of the structure of .Wav Format that we need to setting is:

- *Wave-audio Format: PCM (Pulse-Code Modulation)* [Pulse-Code Modulation].
- *Channel Type: mono.*
- *Sample Rate: 44,100 Hz.*
- *Avgbytepersec: BlockAlign * Sample Rate.*
- *BlockAlign: (Channel * BitsPerSample) / 8.*
- *BitPerSample: 16 bit.*

where the Channel type is 1 which is presented mono; Avgbytepersec is the number of bytes per second; BlockAlign presents the number of byte per sample; Bitpersample is the bit number of quantization per sample.

The Sample Rate of 44,100 Hz is referring to the sampling theorem [Nyquist

Rate] described as follow:

$$f_S > 2f_B \qquad (3.1)$$

where the *fs* is the sample rate; f_B is the biggest original frequency.

We utilize the sound card to catching the heart signal liked as the voice. The sound that a human can hear is roughly from 20 Hz to 20,000 Hz. Hence, according to the sampling theorem that we need to setting the 20,000 Hz to 44,100, or the signal that we sample will has the aliasing phenomenon [Aliasing] illustrated as below:

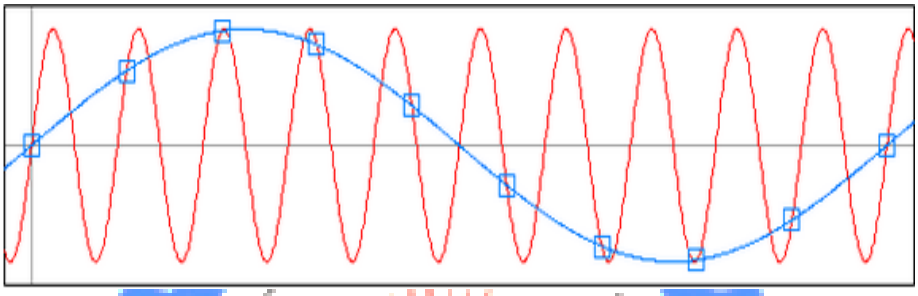

Figure 3-22 Aliasing Phenomenon [Aliasing]

The **Figure 3-22** illustrates the incorrectly sample positions because the sample rate is not enough. The RIFF is a specification proposed by Microsoft for the storage of multimedia files. A RIFF file starts out with a file header followed by a sequence of data chunks. A WAVE file is often just a RIFF file with a single "WAVE" chunk which consists of two sub-chunks: a "fmt " chunk specifying the data format and a "data" chunk containing the actual sample data. Usually, Call this form the "Canonical form" described as follow [Wilson, 2003]:

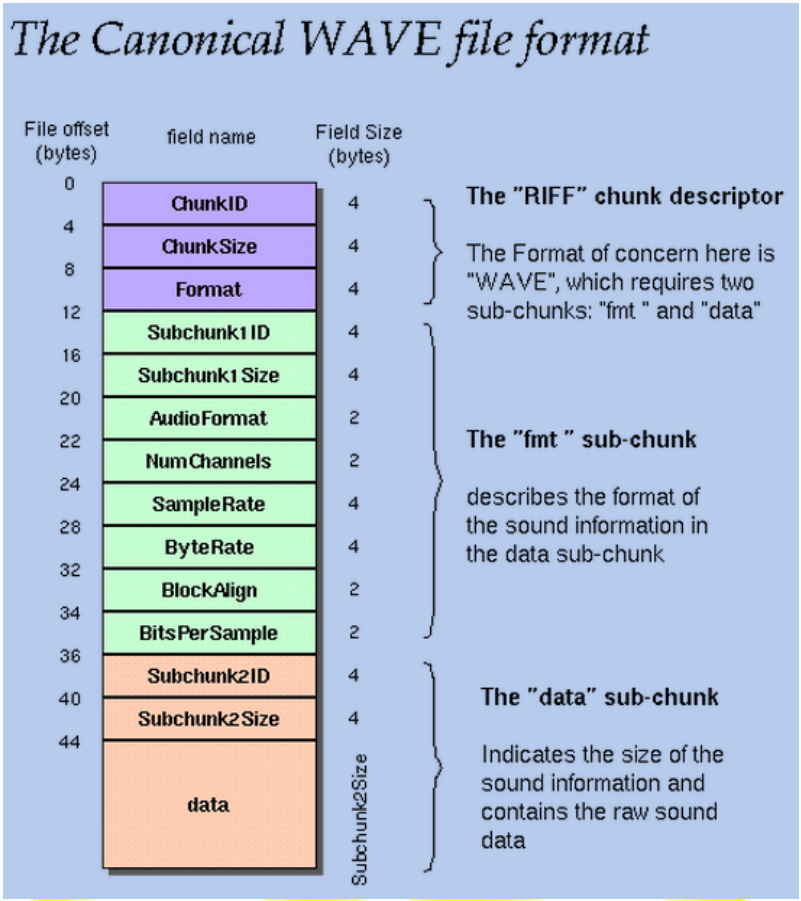

Figure 3-23 Canonical WAVE File Format [Wilson, 2003]

where

- *ChunkID: Contains the letters of "RIFF" in ASCII form.*
- *Chunk Size: This is the size of the entire file in bytes minus 8 bytes for the two fields not included in this count: ChunkID and ChunkSize, and the Chunk Size can calculate as:*

$$4 + (8 + SubChunk1Size) + (8 + SubChunk2Size) \qquad (3.2)$$

- *Format: Contains the letters "WAVE".*

The "WAVE" format consists of two subchunks: "fmt " and "data". The "fmt " subchunk describes the sound data's format:

- *SubChunk1ID: Contains the letters "fmt ".*
- *SubChunk1Size: This is 16 for PCM. It is the size of the rest of the Subchunk*

which follows this number.

- *AudioFormat: Refers to form of compression. Usually, it is PCM = 1.*
- *NumChannels: The channel type, for example, the Mono = 1, the Stereo = 2, etc.*
- *SampleRate: 8000, 44100, etc.*
- *ByteRate:*

$$ByteRate == (SampleRate * NumChannels * BitsPerSample) / 8 \quad (3.3)$$

- *BlockAlign: Presents the number of byte per sample described as below:*

$$BlockAlign == NumChannels * BitPerSample / 8 \quad (3.4)$$

- *BitsPerSample: 8 bits = 8, 16 bit = 16, etc.*

The "data" subchunk contains the size of the data and the actual sound:

- *SubChunk2ID: Contains the letters "data"*
- *SubChunk2Size: This is the number of bytes in the data described as below:*

$$SubChunk2Size == NumSamples * NumChannels * BitsPerSample / 8 \quad (3.5)$$

- *Data: This is the actual sound data.*

Afterward, we can understand the practical application via an example as below:

Table 3-2 Hexadecimal Numbers of Practical WAVE [Wilson, 2003]

As an example, here are the opening 72 bytes of a WAVE file with bytes shown as hexadecimal numbers:

```
52 49 46 46 24 08 00 00 57 41 56 45 66 6d 74 20 10 00 00 00 01 00 02 00
22 56 00 00 88 58 01 00 04 00 10 00 64 61 74 61 00 08 00 00 00 00 00 00
24 17 1e f3 3c 13 3c 14 16 f9 18 f9 34 e7 23 a6 3c f2 24 f2 11 ce 1a 0d
```

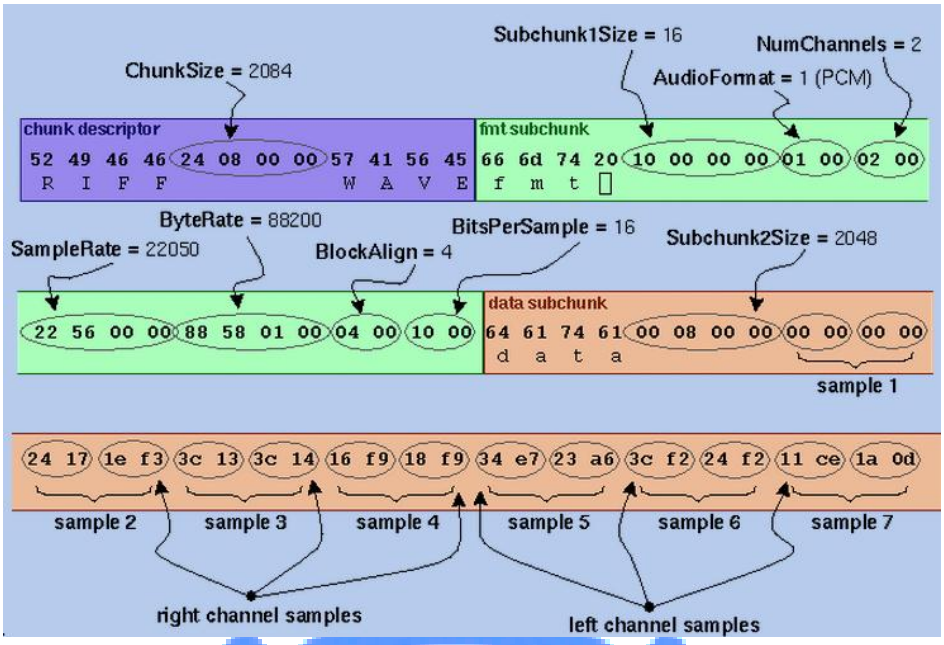

Figure 3-24 Arrangement of RIFF [Wilson, 2003]

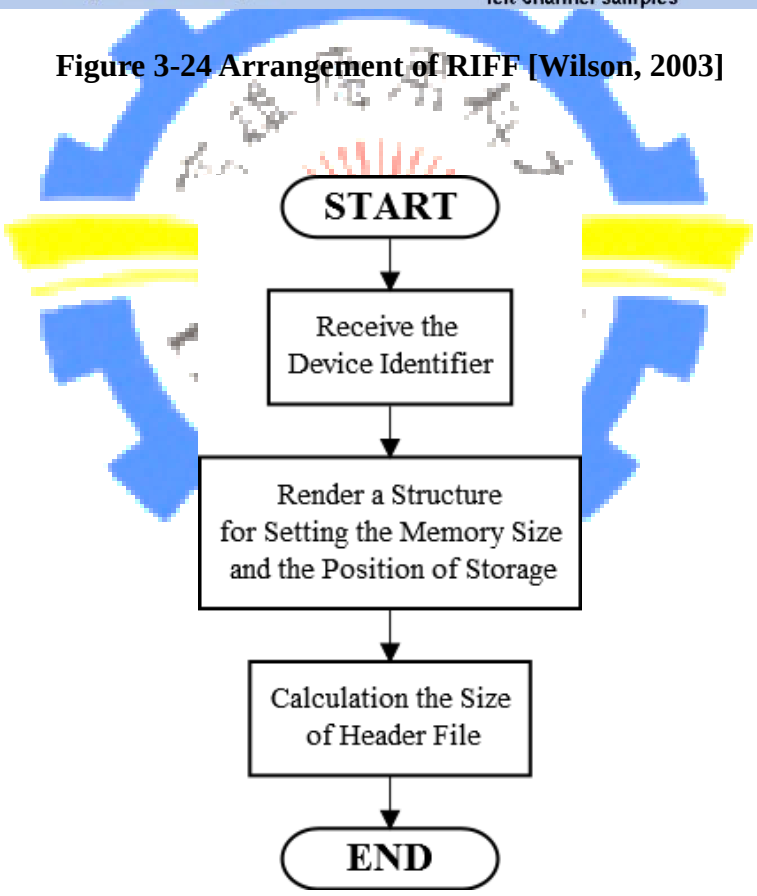

Figure 3-25 Process of WaveInPrepareHeader

The **Figure 3-25** shows the Process of WaveInPrepareHeader function. That allocate a buffer for the wave data, and the memory size (buffer) can measure via:

$$Memory\ Size = SamplePerSecond \times Recording\ Time(sec.)$$

$$\times BytesPerSample. \qquad (3.6)$$

The size of Header refers to a structure which is called the WAVEHDR. This structure defines the header used to save the waveform-audio information for RIFF.

The WaveInAddBuffer function is used to send buffers to device driver. As the buffers are filled with recorded waveform-audio data, the application is notified with a window message, callback message, thread message, or event, depending on the flag specified when the device was opened. This function can use to avoid the situation of data lost. Especially, the data could be lost when the filled buffer will be opened by WaveInStart function. The WaveInStart function is used to start the device for recording the audio. Finally, the WaveInClose function is used to close the device for stopping record.

3.4 QRS Detection

The **Figure 3-26** illustrates the process of QRS detection. Before we detect the QRS wave, we need to know some knowledge about drawing the wave. Accuracy of the sample decides whether the detail of wave can appear or not. The detail information for ECG signal is important because the clinicians need to know the PQRST wave for diagnosis. The **Figure 3-27** illustrates how many sample times is the system do per second. More sample rate we set, and the more accuracy we obtain. Hence, if no memory restriction, the higher sample rate will be better. The **Figure 3-28** shows the sample resolution. That is relevant to the BitPerSample which described as upon.

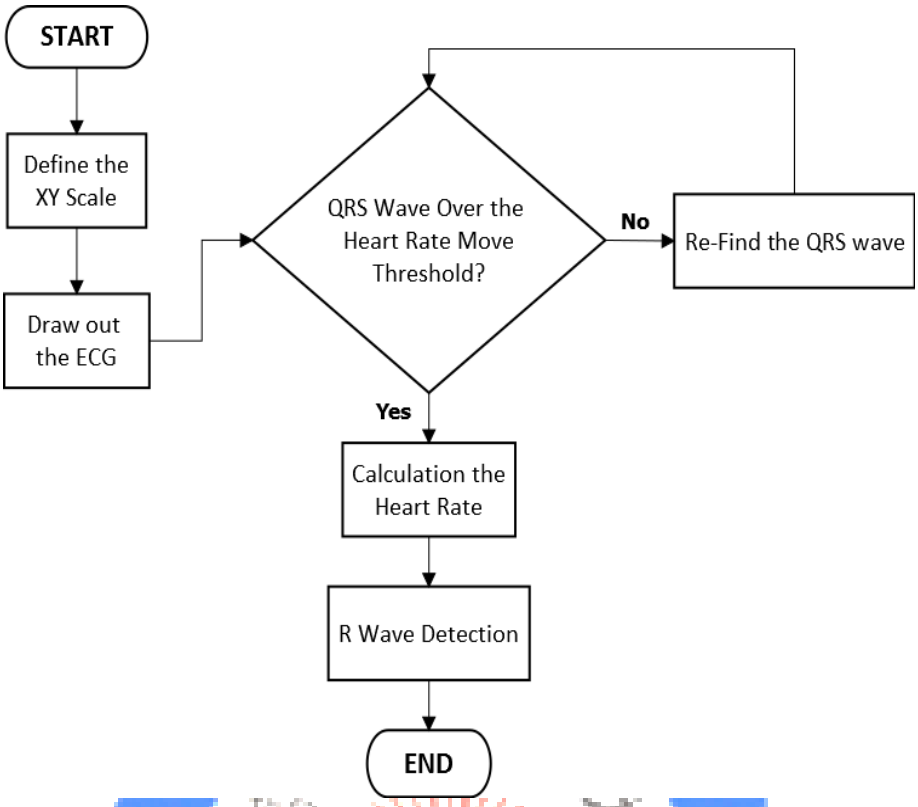

Figure 3-26 Flow Chart of QRS Detection

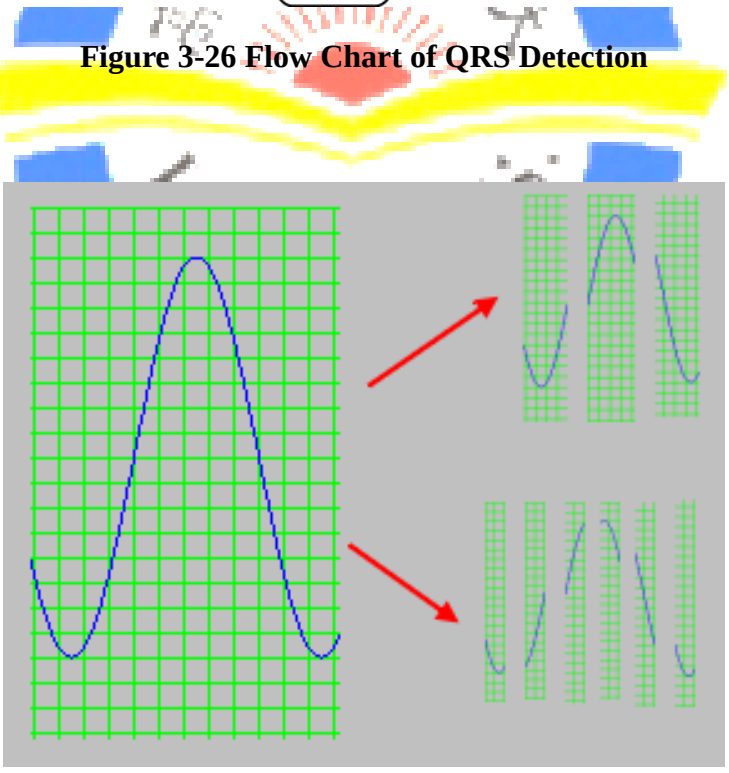

Figure 3-27 Scale of Sample Rate

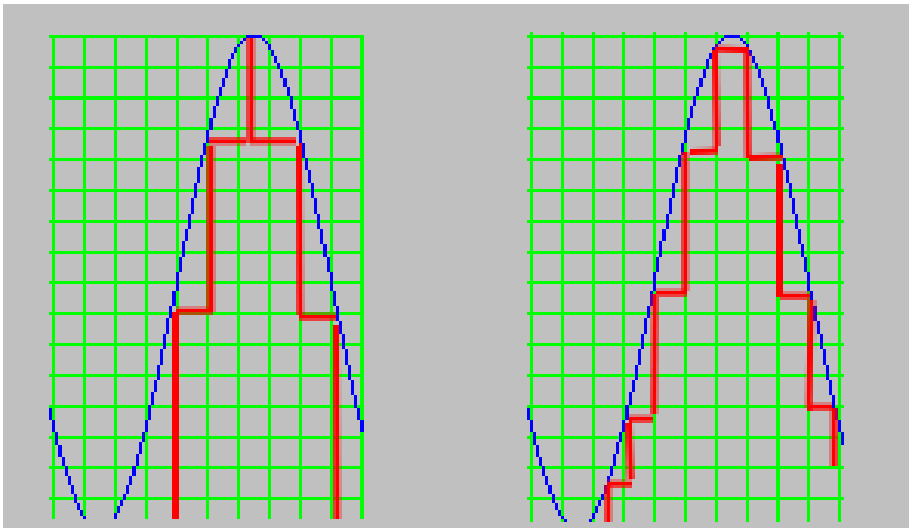

Figure 3-28 Scale of Sample Resolution

If the sample rate is relevant with x axis, and the sample resolution is relevant with y axis. Therefore, the y axis presents the amplitude of signal (or resolution of sound quality). In the other words, that refers to how many data per sample. More sample resolution will have more detail information for strength.

Now, if we want to display the signal clearly on the screen, we need to know how many data you receive and define your x scale clearly. The **Figure 3-29** shows the data you receive every second. So, in the next step, we will introduce how to know the data you received per second and define the y scale further. Eq. (3.7) expresses stream of current received data which is up to *BL* described as below:

$$R_{SC} = R_C \ mod \ BL \qquad (3.7)$$

where the R_C is current received data, and the *BL* is buffer length.

Afterward, we substitute Eq. (3.7) into:

$$RA = INT(\frac{R_{SC}}{BL} \times Screen\ Width) \qquad (3.8)$$

where the *RA* is arrange $R_{SC,}$ *Screen Width* is the width of display screen.

We arrange the R_{SC} with *BL* into a percent of screen width. So, the *RA* is a multiple of *Screen width*.

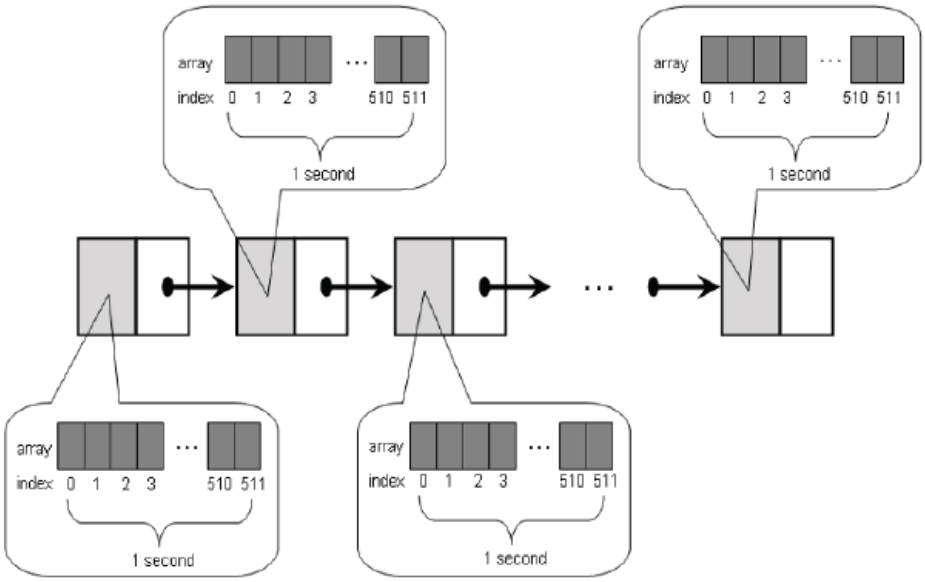

Figure 3-29 Data Link List [Wang, 2008]

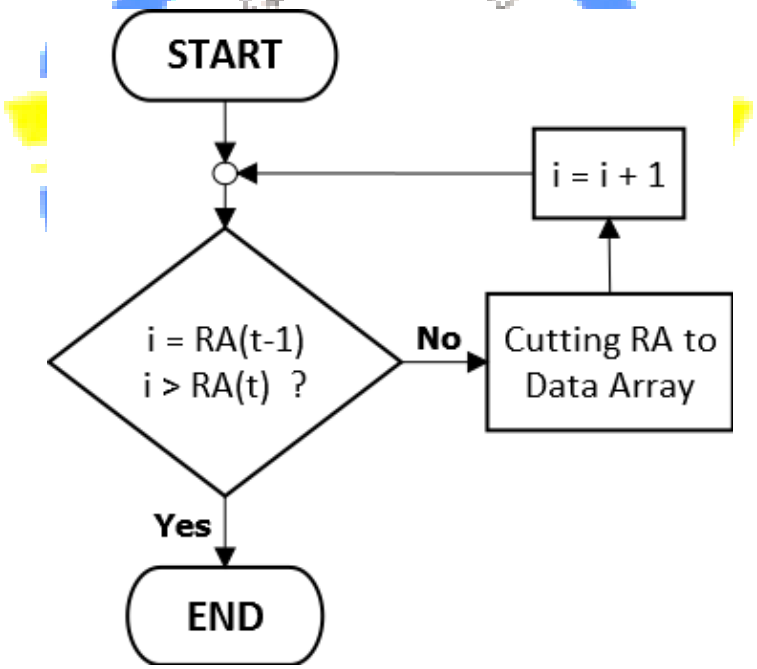

Figure 3-30 Arrange the Data Array

The **Figure 3-30** illustrates the process of arrangement the data array. For cutting out the data array, we need to know where is the position of start of data and position of end of data described as below:

$$R_{DS} = INT\left(\frac{index}{Screen\ Width} \times \frac{Buffer\ Length}{2}\right) \quad (3.9)$$

$$R_{DE} = INT\left(\frac{index+1}{Screen\ Width} \times \frac{Buffer\ Length}{2}\right) \quad (3.10)$$

where the R_{DS} is the position of start of received data, the R_{DE} is the position of end of received data, *index* is the *i* of **Figure 3-30**.

Using the Eq. (3.9) and Eq. (3.10), we arrange the data into a trim data array which likes the **Figure 3-29**.

The scale of x axis is finished by upon method. Afterward, the scale of y axis just employs the BytesPerSample and the scale of x axis to implement.

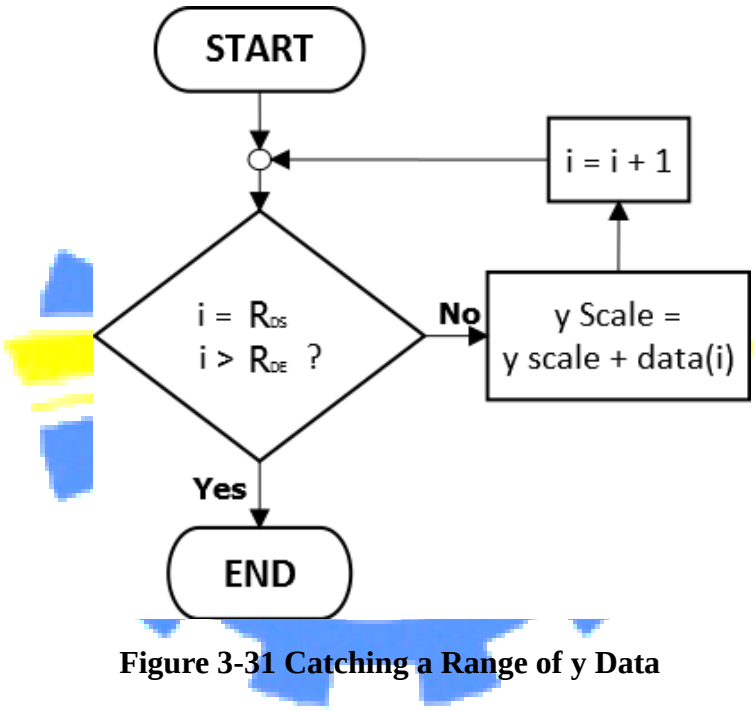

Figure 3-31 Catching a Range of y Data

The **Figure 3-31** shows the caught data of y from R_{DS} to R_{DE}. Afterward, we trim the y scale to an average of *y scale* illustrated as:

$$y\ scale = \frac{y\ scale}{(R_{DS} - R_{DE})}. \quad (3.11)$$

Substituting the Eq. (3.11) into Eq. (3.12) for acquiring the Y_{PP}:

$$Y_{PP} = \frac{y\ Scale}{2^{16}} \times Screen\ Height. \quad (3.12)$$

where Y_{pp} is the practical position of y data on the screen, 2^{16} is the BytesPerSample's value which presents the bytes per sample.

We build the x and y axis successfully. So, we can draw out the ECG wave according to the relation of last point and next point to draw out the wave.

For detection where is the QRS complex, we need to find the R wave first. The R wave is the most important characteristic on ECG because others wave have a relationship with it. The Eq. (3.13) illustrates when the Y_{PP} is over the right of

$$Y_{PP} > TriggerLevel \times \frac{Screen\ Height}{2} \quad (3.13)$$

Eq. (3.13) will enter the sub-function edge_trigger. The move threshold which is illustrated in **Figure 3-26** will follow the maximum y data to re-define the threshold for ensuring the R wave could be detection. The edge_trigger sub-function is used for the heart rate detection. Using the Eq. (3.14) can obtain the heart rate per minute.

$$Heart\ Rate = INT(\frac{60}{Recording\ Time} \times \frac{Screen\ Width}{Index - Prev\ Index} \times 10)/10 \quad (3.14)$$

3.5 R-R Interval Detection

Upon section, we introduced how to detection the R-wave. Here, we will use this method to detection the R-R interval further. There is shown the process of R-R interval detection described as follow:

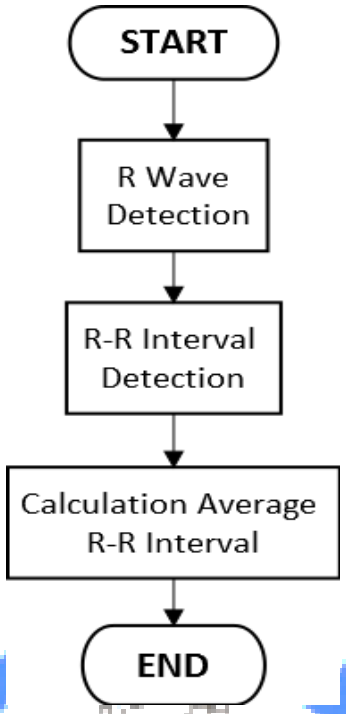

Figure 3-32 Process of R-R Interval Detection

We search out two points of R to define the interval. Via the Pythagorean theory, we measure out the interval illustrated as below:

$$RR\ Interval = \sqrt{(X(i) - X(i-1))^2 + (Y_1 - Y_2)^2} \quad (3.15)$$

3.6 HRV Detection

By searching out the interval in a row up to 5 intervals, use these to obtain the average R-R interval. Employing the 10% average of R-R interval described as **Figure 3-33** to define a range of threshold can detection the abnormal heart rate. If the R-R interval overs this 10% range, the system will show the "danger" to warning. Otherwise, the system will express the "OK".

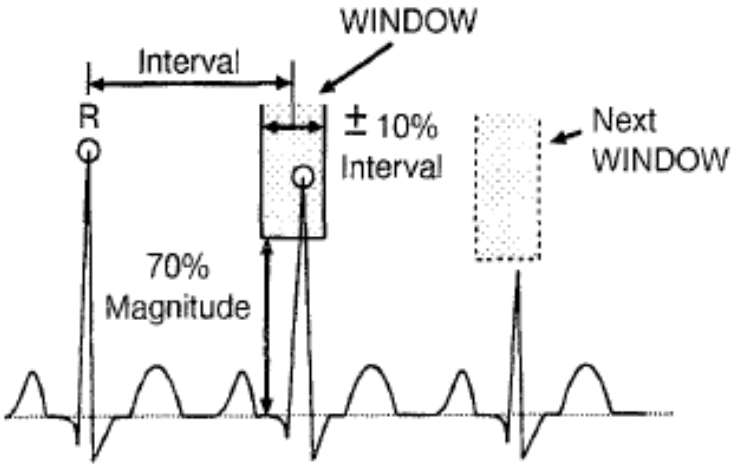

Figure 3-33 Define 10% Average of R-R Interval [KOHAMA et al., 1999]

In 1999, the [D'Addio et al., 1999] proposed a method to judgment the HRV symptom which is the visual method. The **Figure 3-34** illustrates some result consisted of two HRV data.

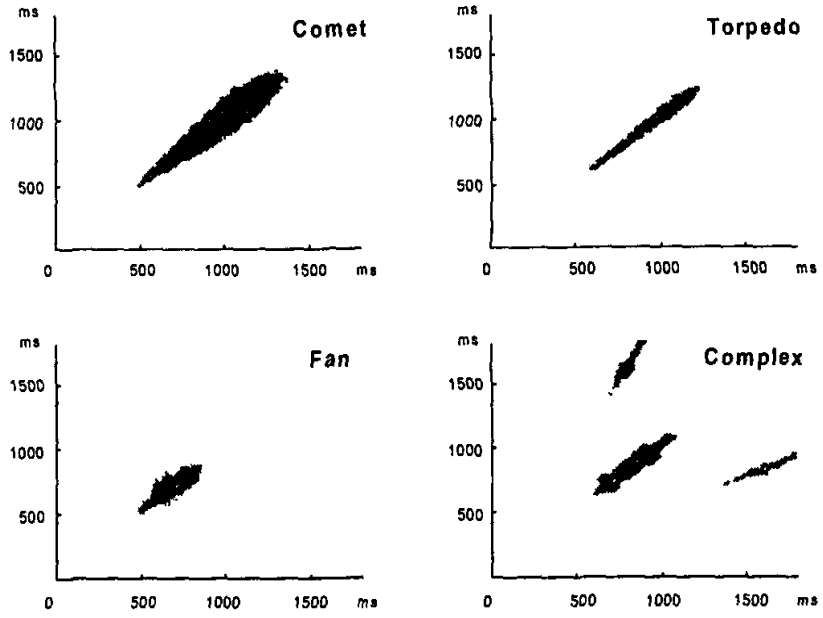

Figure 3-34 Visual Diagnosis Method of HRV

The Comet form is the normal patient, Torpedo form is the patient of severe coma, Fan form is the patient of Irreversible Apneic Coma (IAC), and the Complex form is the patient of severe coma.

3.7 Extended Application on MSP430

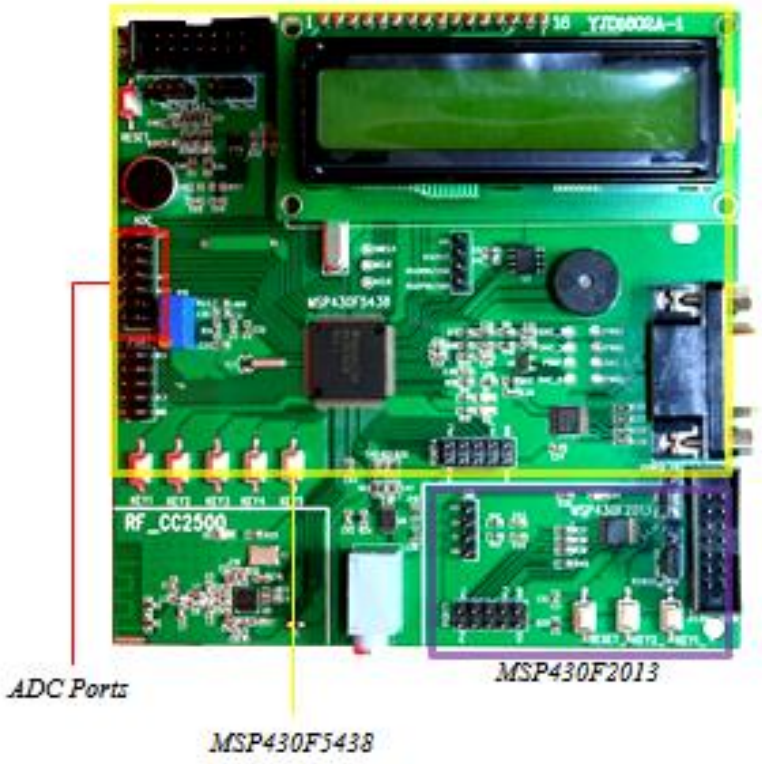

Figure 3-35 MSP430F5438 EVM

The MSP430F5438 described on **Figure 3-35** is very nice platform because it has some advantage for ECG detection illustrated as follow:

- *Ultralow Power Consumption.*
  - *Support up to 4 levels LPM (The highest level: 1.69μA at 3.0V with Fast Wake-Up).*
- *12-Bit Analog-to-Digital (A/D) converter, and four channel conversion mode can selection.*
- *Sample rate up to 200ksps.*

Considering the convenience and practicality, the Holter [Segura-Juarez et al., 2004] is a trend. So, the advantage that I listed on upon is important. For example, the long-term recording of ECG is a basically demand. The **Figure 3-36** is the Low Power Mode (LPM) which function included in MSP430.

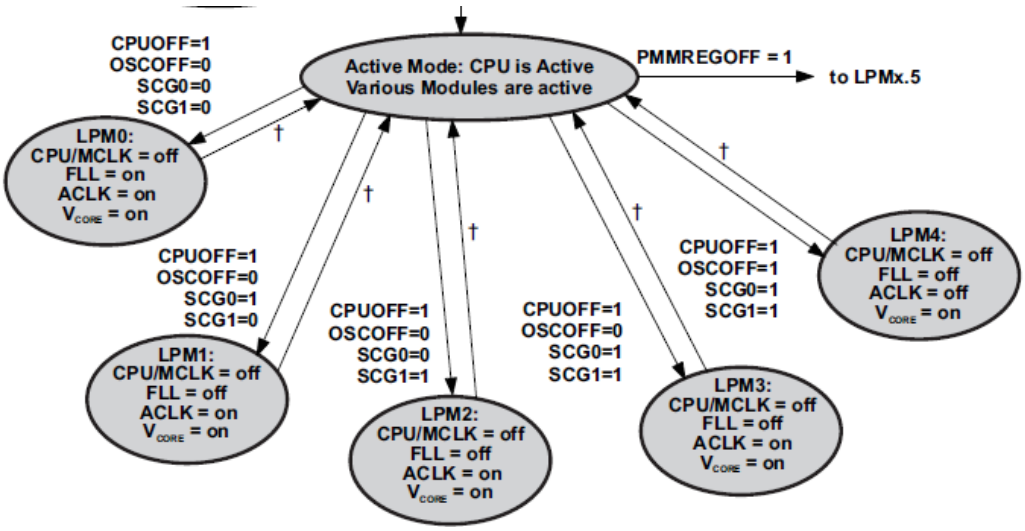

Figure 3-36 Low Power Mode

In the MSP430F5438, the LPM has the four classes which can be selected by you. Each LPM is expressed how many function is closed, for example, the LPM4 disables CPU and all clocks and only keep the core voltage to avoid the memory volatile.

The 12 bit A/D converter has the high sample resolution. That make sure the data could express completely. In MSP430, the A/D converter has to select the channel conversion mode. These channel conversion mode are:

- *Signal-Channel Signal-Conversion Mode*
- *Sequence-of-Channels Mode*
- *Repeat-Signal-Channel Mode*
- *Repeat-Sequence-Channel Mode*

Because the ECG signal is an analog sequence signal, [Chang, 2004] expresses the fourth type which can sequence sample quickly. The repeat-sequence-channel mode is described as follow:

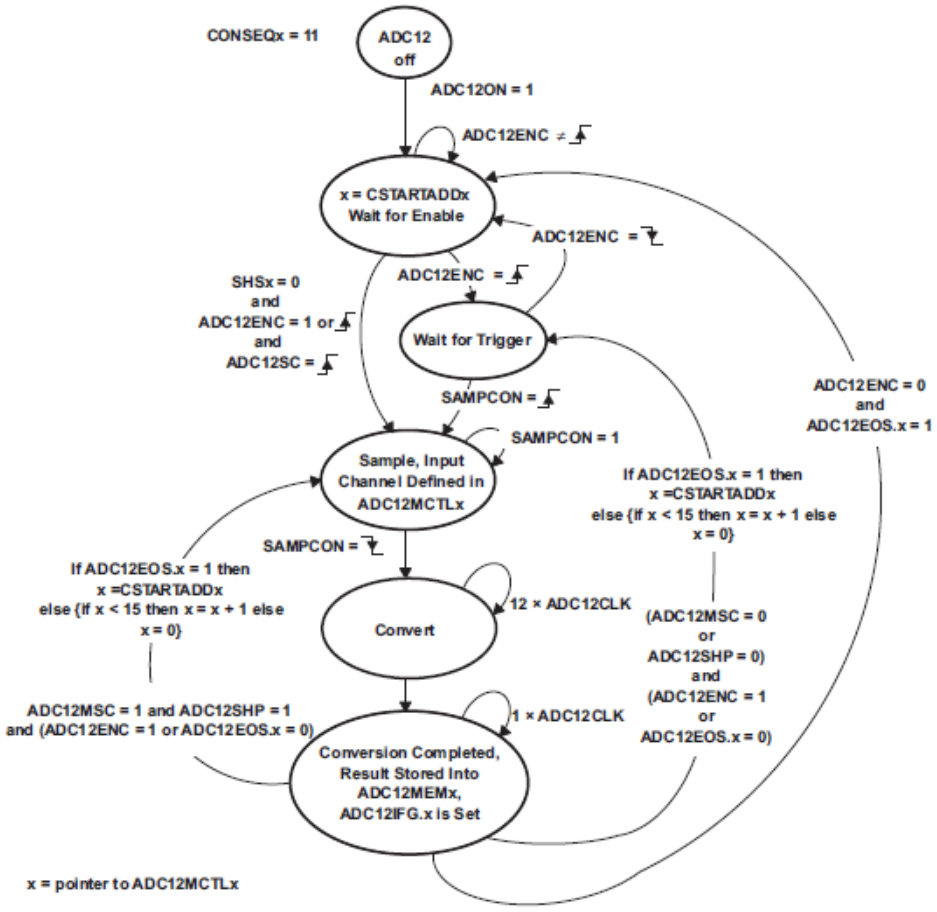

Figure 3-37 Repeat-Sequence-Channel Mode

This type can sequence sample and conversion for multiple sequence signals. If the conversion act is finished, the MCU will set ADC12IFGx, and the conversion data will store in ADC12MEMx.

CHAPTER 4

SIMULATION AND RESULTS

This chapter will introduce each experimental results further. The **Figure 5-1** shows the system window.

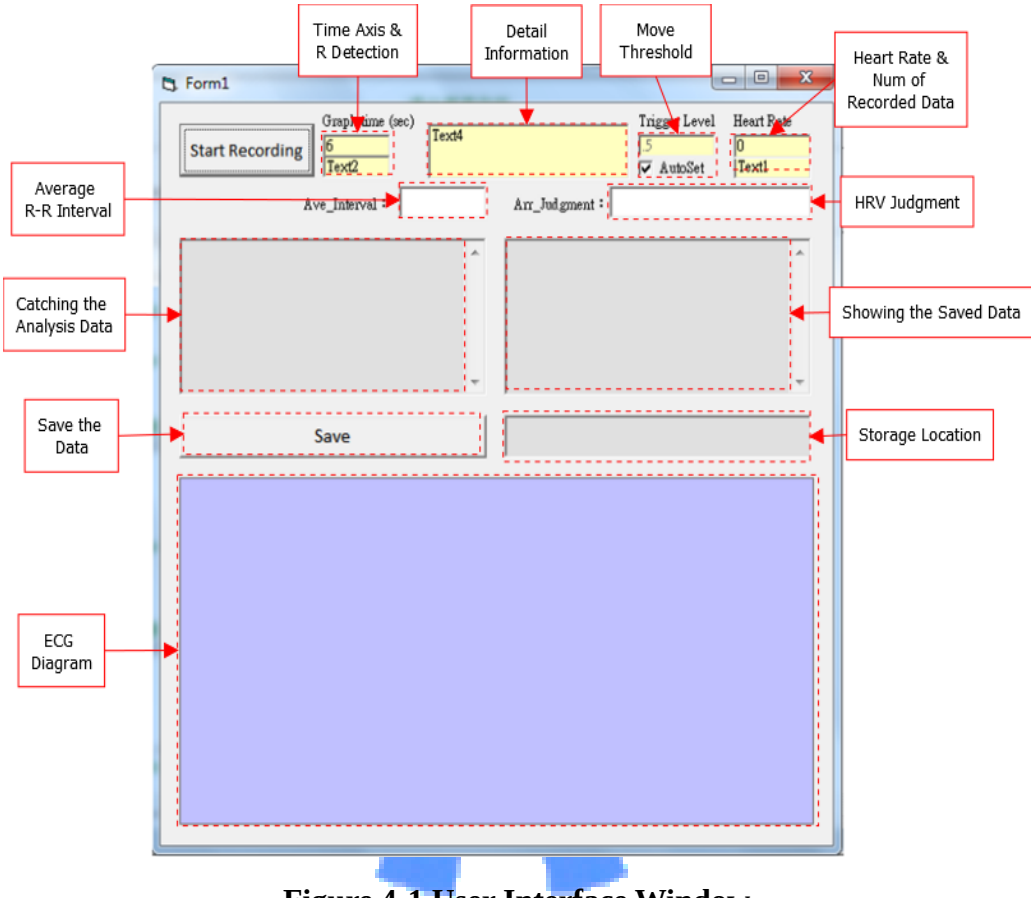

Figure 4-1 User Interface Window

4.1 Hardware Configuration

The **Figure 4-2** is the main measurement circuit for ECG, and the sub circuit will introduce later. The block wire which is located on below of circuit is the negative electrode, the red one is positive electrode, and the blue one is the body electrode.

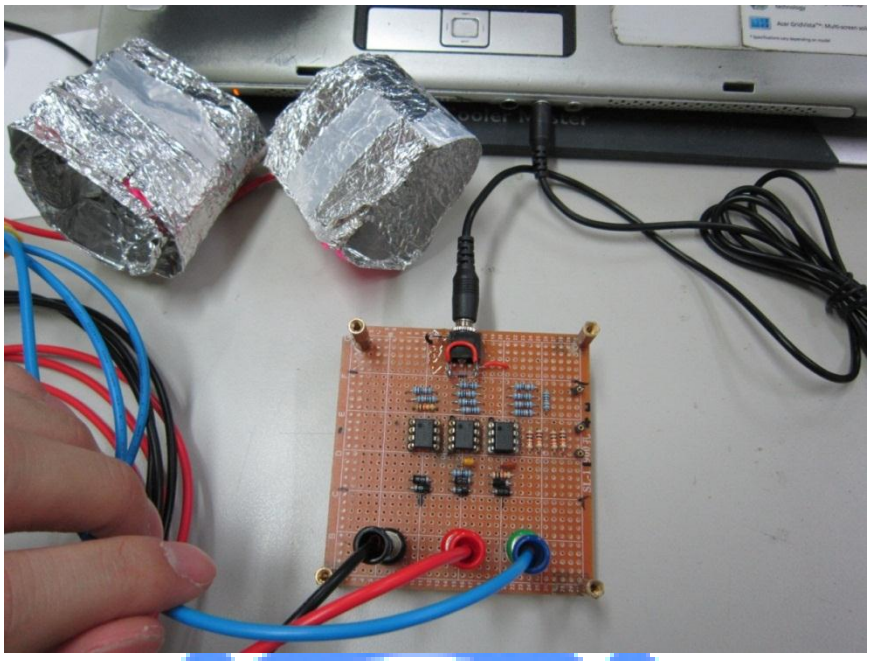

Figure 4-2 Main ECG Measurement Circuit

The Aluminum Foil Artifice (AFA) described in **Figure 4-2** is used to increase the stability and convenience. Due to the coin measurement need to glue the electrodes on chest which increases the inconvenience greatly for patient. We proposed a method using the AFA to measurement the ECG signal. That can increase the conductive area and make the signal stable described in **Figure 4-3** and **Figure 4-4**.

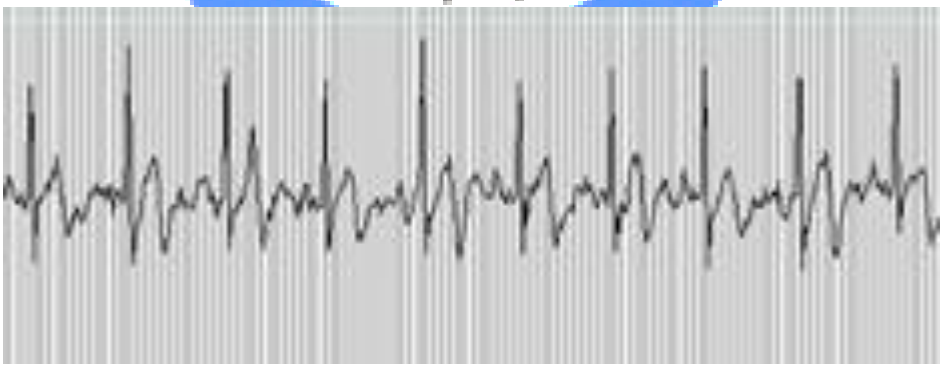

Figure 4-3 ECG of Aluminum Foil Artifice

Figure 4-4 Connection of Aluminum Foil Artifice

The **Figure 4-5** illustrates the effect for Sallen-Kay LPF where upon this figure is EMG noise of ECG, the below one is the filtered ECG.

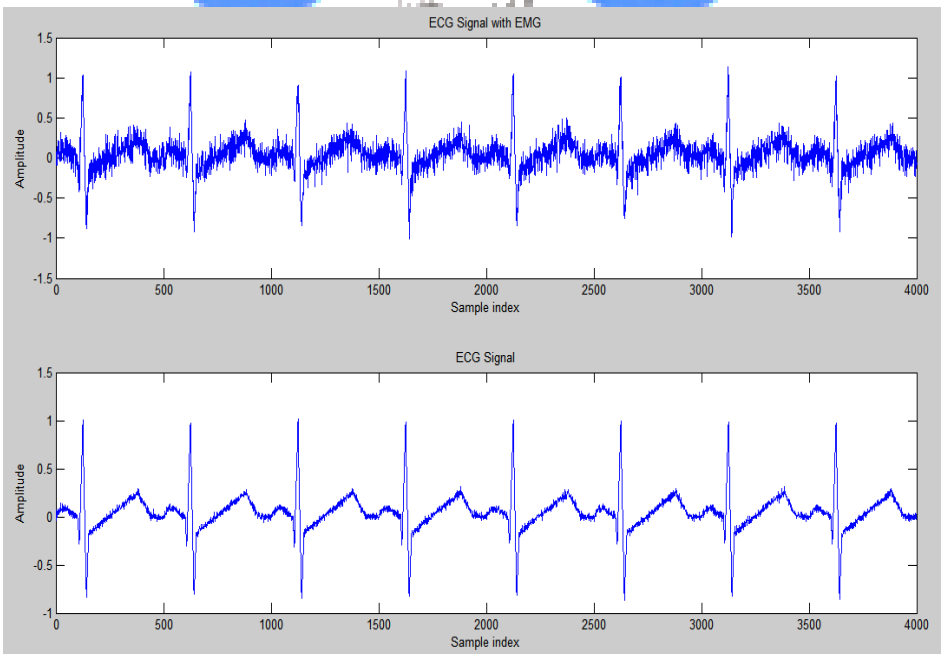

Figure 4-5 Effect on Sallen-Kay LPF

We show the 60 Hz interference. Our low-pass filter is setting on 50 Hz. In the normal situation, if you don't close to transformer too much described in **Figure 4-7**, the 60 Hz noise will not interfere.

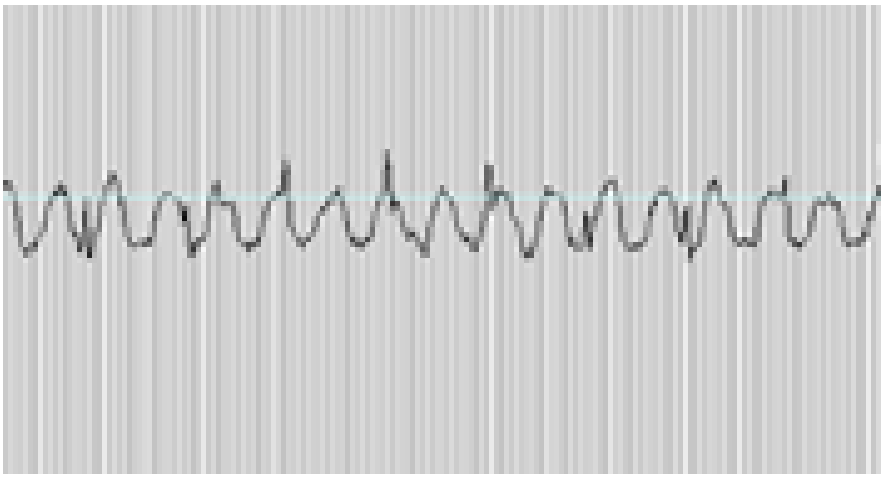

Figure 4-6 60 Hz Interference on AFA ECG

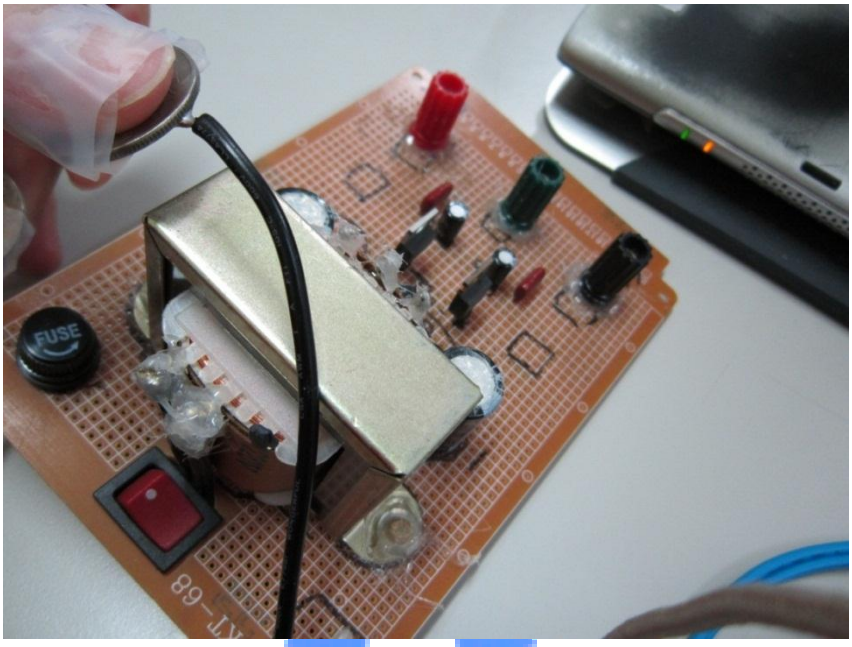

Figure 4-7 Electrode too Closes to the Transformer

The **Figure 4-8** expresses the effect of Sallen-Kay BPF.

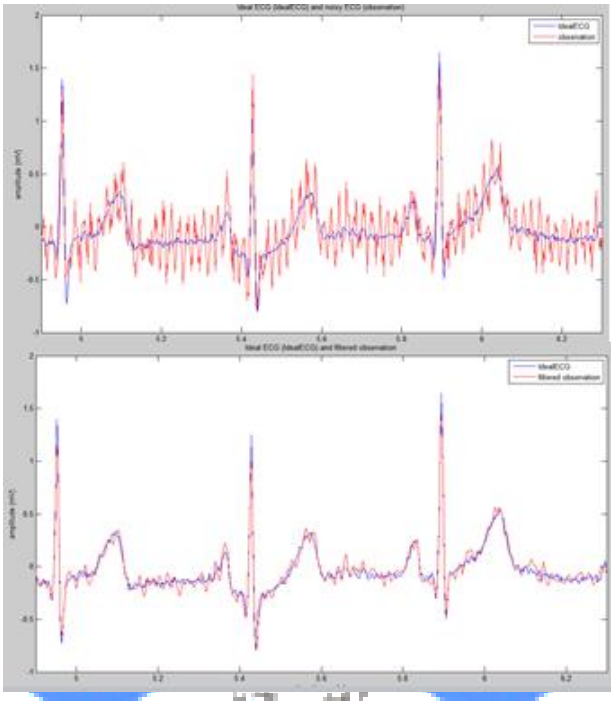

Figure 4-8 60 Hz Interference plotted using Matlab

4.2 Software Configuration

The **Figure 4-9** illustrates R detection on ECG machine.

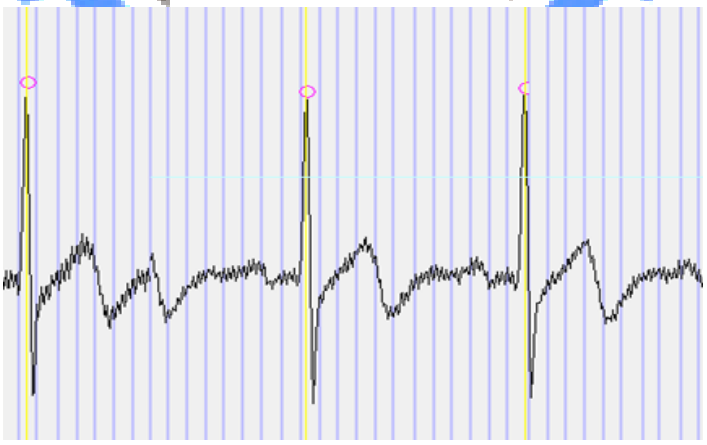

Figure 4-9 R Detection

The **Figure 4-10** shows the practical R-R interval. The red wire is which we use to measurement the R-R interval between R-R.

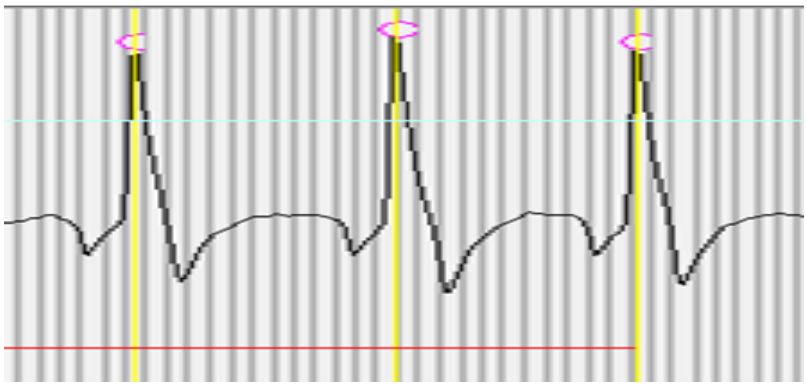

Figure 4-10 R-R Interval

The **Figure 4-11** shows the practical HRV detection.

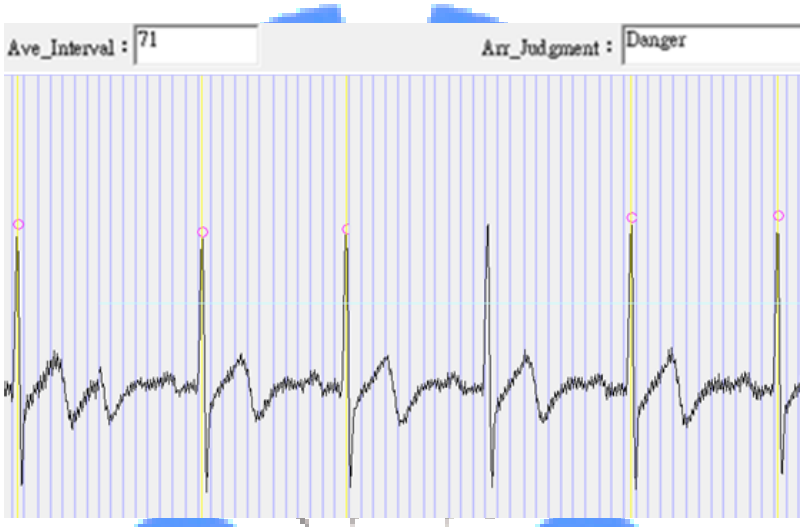

Figure 4-11 HRV Detection

4.3 HRV Data Analysis

The **Figure 4-12** illustrates the HRV analysis within 10 minutes. The blue wire is the real HR, and the block is mean value.

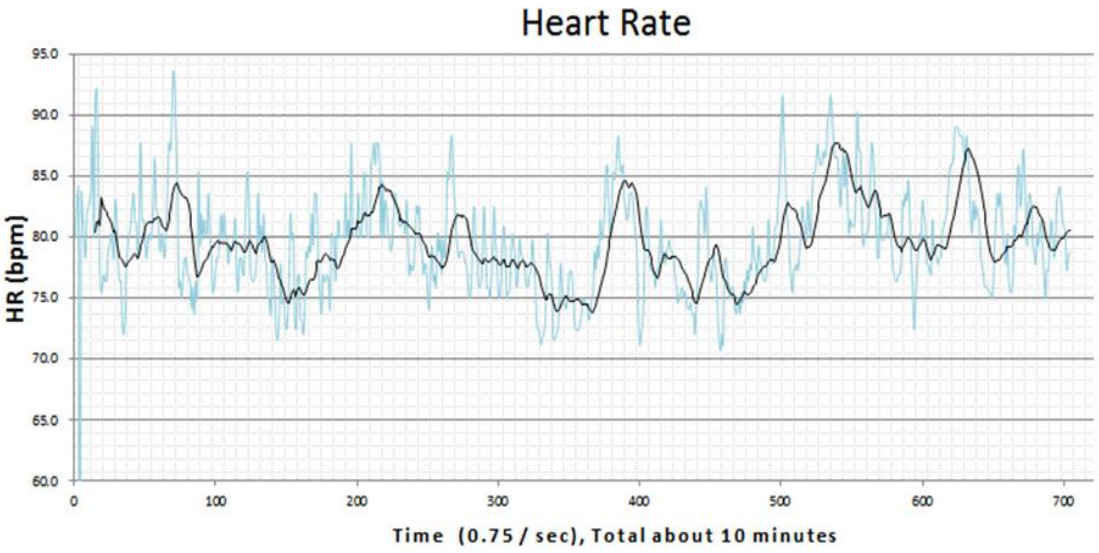

Figure 4-12 HRV Plot

Employing this diagram, we can find the heart rate varying. Maybe this analysis could use to as the polygraph to finding the ruffian. Afterward, we want to analysis the HRV further. So, the **Figure 4-13** is the interval time per R-R interval (RRI).

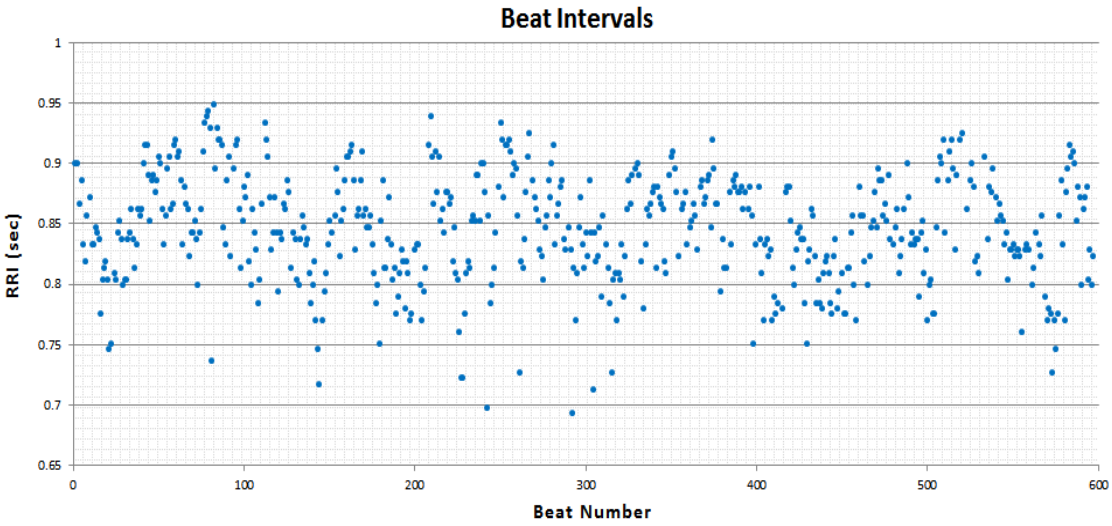

Figure 4-13 R-R Interval Time

For employing the visual diagnosis method of HRV, the data of **Figure 4-13** is necessarily. The **Figure 4-14** use two data of RRI time to observe the HRV. In this figure, we can realize that it is a comet form.

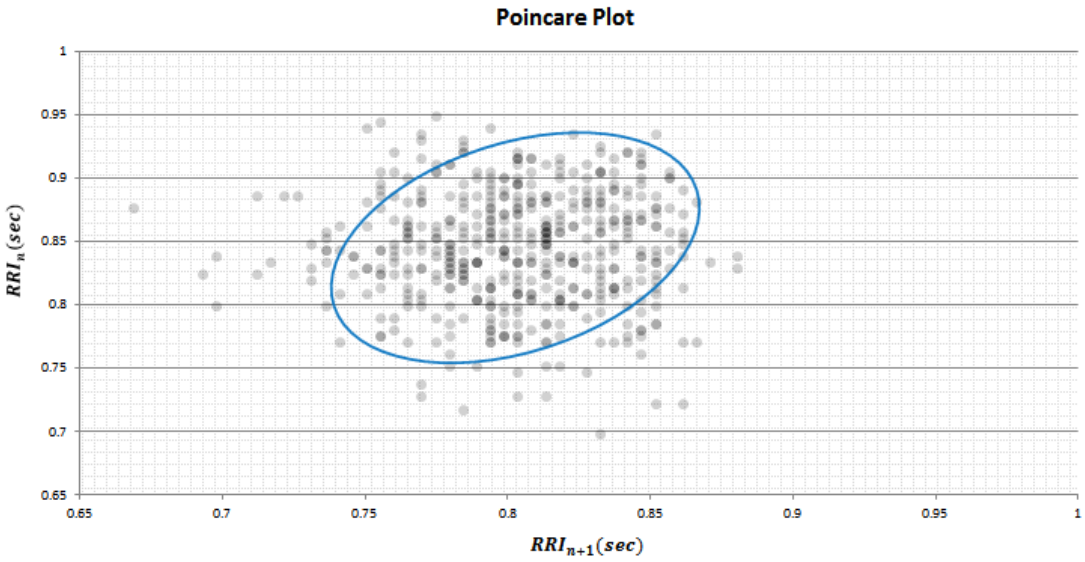

Figure 4-14 Poincare Plot

Among the HRV analysis method, the Standard Deviation of the all NN (or RR) interval (SDNN) is usually utilized to judgment a patient which has a higher probability of SCD. The statistical method is described as follow:

$$\mu = \frac{1}{N}\sum_{i=1}^{N} RRI(sec)_i \qquad (4.1)$$

$$\sigma = \sqrt{\frac{1}{N}\sum_{i=1}^{N}(RRI(sec)_i - \mu)^2} \qquad (4.2)$$

where μ is average value, and σ is SDNN.

The **Table 4-1** shows the *RRI* sequence data about 5 minutes. We calculate my SDNN that is 0.115737822. This value means the variability extent of *RRI*. If this value is large presenting this patient has a lower probability of SCD. Otherwise, the patient has a higher one. That is because the more SDNN presents the more data transform among the heart. The higher one can help the heart to adapt the change of physical environment [WithYourVoice, 2004].

Table 4-1 RRI Sequence Data

RRI [n]
0.75
0.738916
0.706714
0.738916
0.754717
0.787402
0.771208
0.771208
0.803213
0.803213

In chapter 1, we know the overwork which affects the heart more, and that will cause the SCD. Now, we want to know more factors which affect the heart. Employing the Taguchi Methods [Chou, 2011] to observe the SDNN, we can acquire which one will influence the heart. We list a L4 Orthogonal Array [Chou, 2011] and the control factor that we want to observe described as below:

Table 4-2 Control Factors

Control Factor	Level 1	Level 2
A (Night or Morning)	1	2
B (Sport? No or Yes)	1	2
C (Food? No or Yes)	1	2

Table 4-3 L4 Orthogonal Array

Experiment No	Factors		
	I	II	I x II
1	1	1	1
2	1	2	2
3	2	1	2
4	2	2	1

Utilizing Orthogonal Array can obtain the least number of experiments. According to this table, the original experiments can down to four times from two cubic. Afterward, he SDNN Orthogonal Array is listed as follow:

Table 4-4 SDNN Orthogonal Array

L4 OA	A	B	C	y	MSD	S/N 比
1	1	1	1	0.04126	0.001702	-27.6894
2	1	2	2	0.03299	0.001088	-29.6324
3	2	1	2	0.04935	0.002435	-26.1343
4	2	2	1	0.03756	0.001411	-28.5055

where y is the SDNN data in view of four condition on **Table 4-2**, and MSD is Mean Square Derivation.

The **Table 4-5** is used to build the diagram which can observe the variation extent described as follow:

Table 4-5 Response Table

RT	A	B	C
1	-28.66088461	-26.9118	-28.0975
2	-27.88330527	-29.0689	-27.8833
max-min	0.777579334	2.157085	0.214147

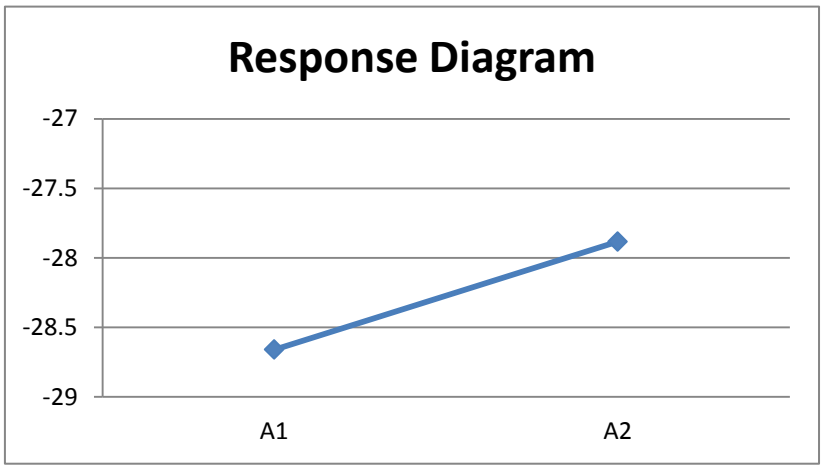

Figure 4-15 Variation Extent of A Factor

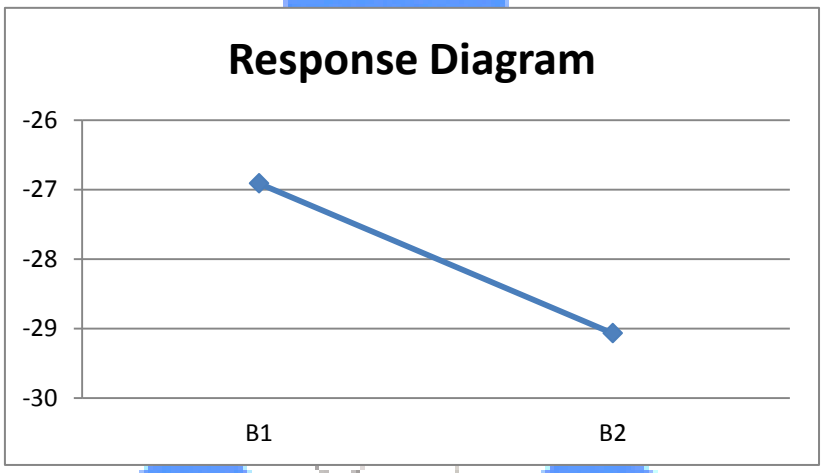

Figure 4-16 Variation Extent of B Factor

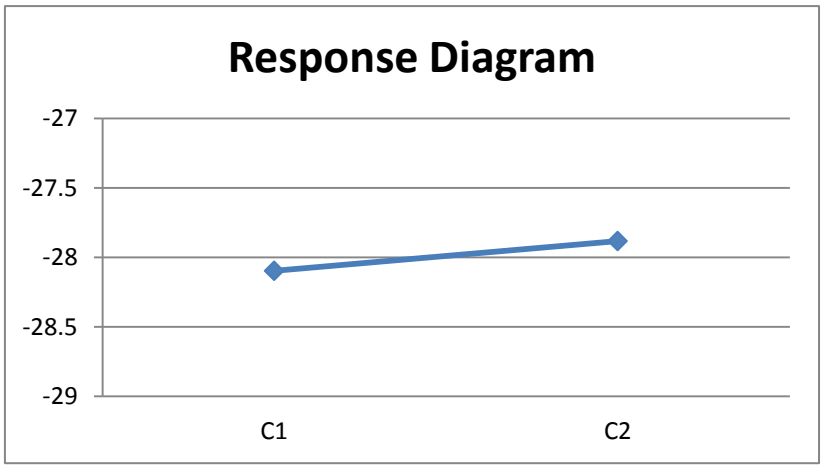

Figure 4-17 Variation Extent of C Factor

Employing these diagram, we can find the higher variation is A and B. The ANOVA (Analysis of Variance) can show the contribution which one is the greatly high illustrated as below:

Table 4-6 ANOVA

Factor	Variance	Degrees of Freedom	Variation	Pure Variance	Rate of Variation	Contribution
A	1.798313222	1				
B	4.653014899	1	4.653015	4.653015	202.9279	0.71615839
C	0.045858789	1				
e	-9.09495E-13	0				
et	0.045858789	2	0.022929	1.844172		0.28384161
T	6.49718691	3		6.497187		1

In ANOVA table, we can find the highest contribution is the B situation, and the highest rate of variation is it too. So, we can realize the sports which have the highest extent of effect. The second is the A (or day and night). Even, the A is not the highest one, but it is an important event too because that expressing the patient is tired at night. Hence, in the future, if we want to search out more effect factor, we can include more control factor inside the Orthogonal Array, and will find much important factor.

In the final, we list the main component which is the off-shelf one, and you will find that is incredible cheap!

- 3 x LF353 - Dual Op-amp (3 x 18 NT).
- Twelve 1% tolerance and 1/4 Watt 100k resistors (12 x 0.3 NT).
- Six 10k resistors (6 x 0.3 NT).
- One 1uF Ceramic capacitance (1 x 4 NT).
- One 0.1uF Ceramic capacitance (1 x 3 NT).
- Six 1N4001 diode (6 x 2 NT).
- One 3.5mm microphone plug (1 x 15 NT).

Besides the ten coins electrodes, that just only costs 94 NT.

CHAPTER 5

CONCLUSION

In this paper, we finished a low cost electrocardiogram (ECG) machine with off-the-shelf components implementing the real-time QRS wave and Heart Rate Variability (HRV) detection. We apply the Sallen-Kay and Notch filter to remove unwanted noises included in signal, and develop a real-time ECG and HRV monitoring system. Via this system we show the QRS wave and the detection result of HRV on this system. Finally, utilizing these ECG information, we analyzes which factor or condition will affect the heart rate. Finally, we employ the Taguchi method to observe the SDNN which will cause the SCD. In the future, we want to combine the ZIGBEE and MSP430 for building the Holter which is a portable ECG machine.

5.1 Future Work for Remote Monitoring

HRV usually occurs on patient which has the arrhythmia. This kind of symptom is not so common. If this symptom occurs quickly and suddenly, the patients will have risk of causing SCD. Therefore, the ECG machine has the requirement to add in the remote monitoring. The ZIGBEE is a good choice because the associated mesh network can be constructed by any readers, and its topology can cope with most environments.

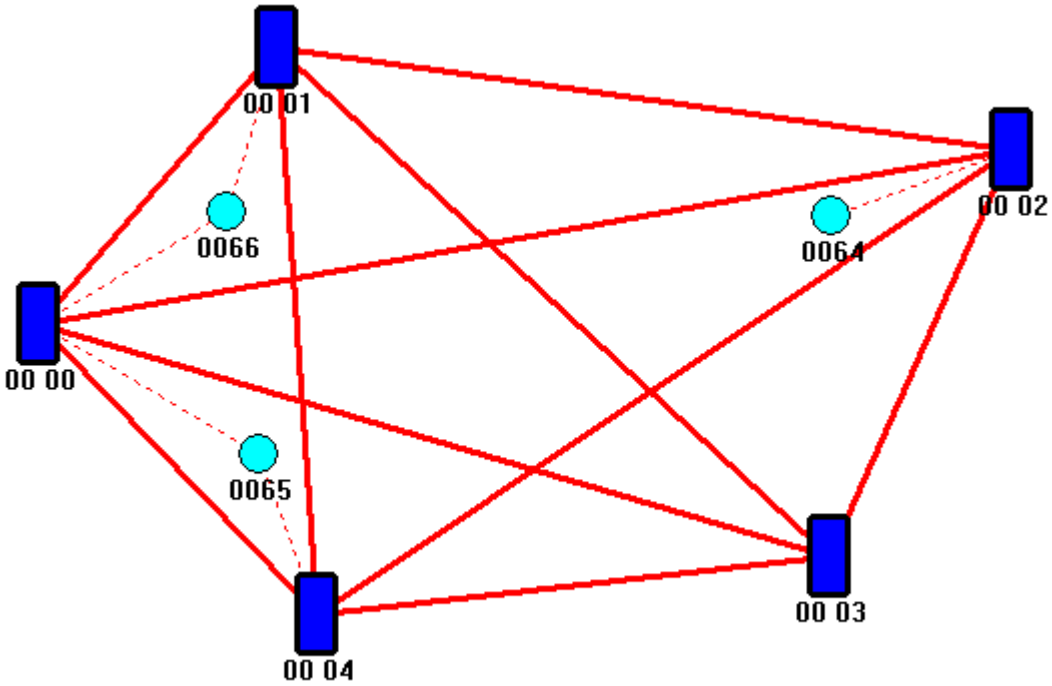

Figure 5-1 Searching the Target by ZIGBEE

The **Figure 5-1** shows the ZIGBEE's sensors which can search the target using readers. For example, there are five readers and three targets. By employing each shortest distant which is between readers and targets on sensor network, we can locate the target patient.

REFERENCE

[Rusu et al., 2008]

Alex. Rusu, C. Ravariu, "MANUFACTURING AND TESTS OF A MOBILE ECG PLATFORM," *IEEE, Semiconductor Conference*, pp.433-436, 2008.

[Aliasing]

URL: http://en.wikipedia.org/wiki/ Aliasing.

[Sallen-Key, 1999]

T. I. Analysis of the Sallen-Key Architecture, Analysis of the Sallen-Key Architecture, URL:http://www.science.unitn.it/~bassi/Signal/TInotes/sloa049.pdf.

[API]

URL: http://zh.wikipedia.org/zh-tw /Windows_API.

[Blioju, 2010]

G. Blioju, "EKG Through Sound-Card," URL: http://www.edusoft.ro/brain/index.php/brain/article/view/86#.

[Sound Card]

URL: http://en.wikipedia.org/wiki/ Sound_card.

[Chang, 2004]

K. S. Chang, "Design of An Embedded Measurement System for Electrocardiograms And Its Application to Remote Individual Care," Electrical Engineering, National Cheng-Kung University, 2004.

[Chou, 2011]

J. H. Chou, "Optimization Approaches", Lecture Notes and Handouts at the Institute of Electrical Engineering, National Kaohsiung University of Applied Sciences, 2011.

[TRS Connector]

URL: http://en.wikipedia.org/wiki /TRS_connector.

[OKAWA, 2008]

OKAWA, "Engineering Design Utilities," URL: http://sim.okawa-denshi.jp/en/.

[Cardiac Dysrhythmia]

URL: http://en.wikipedia.org/wiki/ Arrhythmia.

[Einthoven's Triangle]

URL: http://en.wikipedia.org/wiki/ Einthoven%27s_triangle.

[Waveform Audio File Format]

URL: http://en.wikipedia.org/wiki/WAV.

[D'Addio et al., 1999]

G. D'Addio, G.D. Pinna, R. Maestri, D. Acanfora, C. Picone, C. Furgi, F. Rengo, "Correlation between Power-law Behavior and Poincar& Plots of Heart Rate Variability in Congestive Heart Failure Patients," *IEEE, Computers in Cardiology*, pp.611-614, 1999.

[Group, 1998]

EnCoded Communications Group, "Low-level wave audio part 3," URL: http://bcbjournal.org/articles/vol2/9810/Low-level_wave_audio__part_3.htm.

[YUMAX, 2010]

YUMAX Inc., "淺談犬隻的竇性心律不整," URL: http://www.yumax.com.tw/article_detail.php?cmode&mode&type1&type2&id=38&pstyle.

[KOHAMA et al., 1999]

T. KOHAMA, S. NAKAMURA, H. HOSHINO, "An Efficient R-R Interval Detection for ECG Monitoring System," *IEICE Trans Inf Syst (Inst Electron*

Inf Commun Eng), pp.1425-1432, 1999.

[Lee, 2007]

H. W. Lee, "The Periodic Moving Average Filter for Removing Motion Artifacts from PPG Signals," *International Journal of Control, Automation, and Systems*, pp.701-706, 2007.

[Lin, 2007]

C. C. Lin, "A Cardiac Health Expert System Based On Electrocardiogram," Electrical Engineering, Tzu Chi University, 2007.

[Luo, 2004]

Z. B. Luo, "The Implementation of Wireless ECG Chip by Using PLL Technique," Electrical Engineering, National Cheng-Kung University, 2004.

[Medical-eLearning, 2012]

Medical-eLearning, "HEART AXIS," URL: http://www.heartaxis.com/.

[Microphone]

URL: http://en.wikipedia.org/wiki/ Microphone.

[Pulse-Code Modulation]

URL: http://en.wikipedia.org/wiki/ Pulse-code_modulation.

[MSDN]

Microsoft MSDN, "Waveform Audio Reference," URL: http://msdn.microsoft.com/en-us/library/windows/desktop/dd743833(v=vs.85).aspx.

[T. I., 2010]

T. I., "MSP430x5xx Family," URL: http://www.ti.com.cn/product/cn/msp430f5438.

[NTHU]

Institute of Biomedical Engineering, "Chapter 5 Physiology Experiments,"

URL:http://upwen.com/html/11_Swf_心電圖_941.html.

[Malmivuo et al., 1995]

J. Malmivuo, R. Plonsey, "Principles and Applications of Bioelectric and Biomagnetic Fields," URL:http://www.bem.fi/book/.

[Nyquist Rate]

URL: http://en.wikipedia.org/wiki/ Nyquist_rate.

[Segura-Juarez et al., 2004]

J. J. Segura-Juarez, D. Cuesta-Frau, L. Samblas-Pena, M. Aboy, "A microcontroller-based portable electrocardiograph recorder," *IEEE Trans Biomed Eng*, pp.1686-1690, 2004.

[Wang, 2008]

Y. D. Wang, "A SMS-based Mobile Electrocardiogram Monitoring System," Biomedical Engineering, National Chiao Tung University, 2008.

[Wilson, 2003]

S. Wilson, "WAVE PCM soundfile format," URL: https://ccrma.stanford.edu /courses/422/projects/WaveFormat/.

[李修誠, 2009]

李修誠, "An Application-Specific Integrated Circuit Design for Physiological Monitoring System," Information and Electrical Engineering, Feng-Chia University, 2009.

[葉倍宏, 2010]

葉倍宏，"第 19 章主動濾波器," URL: http://ir.lib.ksu.edu.tw/bitstream/ 987654321/10721/10/chap19.pdf.

[WithYourVoice, 2004]

WithYourVoice Ltd.，"心率變異數在評估生理變化時的重要性," URL:

http://www.hk.withyourvoice.com/HRV.htm.